BRNO UNIVERSITY OF TECHNOLOGY

VYSOKÉ UČENÍ TECHNICKÉ V BRNĚ

FACULTY OF ELECTRICAL ENGINEERING AND COMMUNICATION

FAKULTA ELEKTROTECHNIKY
A KOMUNIKAČNÍCH TECHNOLOGIÍ

DEPARTMENT OF TELECOMMUNICATIONS

ÚSTAV TELEKOMUNIKACÍ

PROGRAMMABLE DIGITAL MULTI-EFFECT

PROGRAMOVATELNÝ DIGITÁLNÍ MULTIEFEKT

BACHELOR'S THESIS

BAKALÁŘSKÁ PRÁCE

AUTHOR AUTOR PRÁCE	**Bc. Pavlo Shelemba**
SUPERVISOR VEDOUCÍ PRÁCE	**Ing. David Kubánek, Ph.D.**

BRNO 2023

BRNO UNIVERSITY OF TECHNOLOGY
FACULTY OF ELECTRICAL ENGINEERING AND COMMUNICATION

Bachelor's Thesis

Bachelor's study program **Audio Engineering**
specialization Zvuková technika
Department of Telecommunications

Student: Bc. Pavlo Shelemba ***ID:*** 212579
Year of study: 3 ***Academic year:*** 2022/23

TITLE OF THESIS:

Programmable Digital Multi-Effect

INSTRUCTION:

Get acquainted with the properties and parameters of the programmable effect chip Spin Semiconductor FV-1 and with the effects that can be realized by this circuit. Study the possibilities of its control using a microcontroller and data buses. Design the concept of a programmable multi-effect unit in the form of a Eurorack module with suitable user control. If element models are available, verify the function of the unit or its parts by computer simulation. Construct this effect, measure its parameters and compare them with theoretical or simulated ones. Also evaluate the listening properties of the effect.

RECOMMENDED LITERATURE:

[1] HOROWITZ, Paul a Winfield HILL. The Art of Electronics. Third edition. New York: Cambridge University Press, 2015. ISBN 978-0-521-80926-9.
[2] ZÖLZER, Udo. DAFX: Digital Audio Effects. 2nd ed. Chichester, UK: Wiley, 2011. ISBN 978-0-470-66599-2.

Date of project specification: 6.2.2023 ***Deadline for submission:*** 26.5.2023

Supervisor: Ing. David Kubánek, Ph.D.

doc. Ing. Jiří Schimmel, Ph.D.
Chair of study program board

ABSTRACT

This work delves into the topic of embeded digital audio signal processing in the context of modular synthesizers. Its theoretical part provides an overview of the basic terms and components used in modular synthesizers. It explores the design of a digital effect unit based on the programmable effect chip Spin Semiconductor FV-1. It also delves into the possibilities of its digital control using a microcontroller and data buses. It also proposes several analog circuits, including an analog voltage-coltrollable crossfader. The output of this work is a design for a Eurorack audio effects proccessor with suitable user control.

KEYWORDS

Modular synthesizer, Eurorack, Digital effect, Digital Signal Processing, DSP, microprocessor

Typeset by the `thesis` package, version 4.07; `http://latex.feec.vutbr.cz`

ABSTRAKT

Tato práce se věnuje studiu digitálního zpracování signálu (DSP) a jeho implementaci v kontextu vestavěných systémů. Jako základ práce je zvolen digitální signálový procesor Spin Semiconductor FV-1. Cílem je poté sestavení modulu pro platformu Eurorack.

Úvod teoretické části rozebírá teoretické základy potřebné pro úspěšný návrh modulárního syntezátoru. Teorie začíná od fyzikální podstaty zvuku a pokračuje základními stavebními prvky syntezátoru. Vysvětluje také význam řídícího napětí a jakým způsobem umožňuje interakci mezi základními prvky. Běžné bloky syntezátoru jde zkoumat z hlediska čtyř základních komponentů: zdrojů zvuku, modifikátorů zvuku, zdrojů modulace a modifikátorů modulace. Demonstruje dvě rozšířené (avšak ne výhradní) metody jejich propojování. Následně vysvětluje, jak se tyto koncepty překládají do světa modulární syntézy. Poté jsou vysvětleny podrobnosti formátu modulárního syntezátoru Eurorack, kde jsou také uvedeny jeho mechanické a elektrické specifikace. Dále se zabývá základy DSP. Jsou zde rovněž rozebrány dva základní koncepty související s digitálním zpracováním signálu: digitální signály a digitální systémy. Vysvětluje význam digitální reprezentace signálu a prochází základy digitalizace zvuku. Modulární syntezátory Eurorack fungují na bázi analogových napětí, proto je pro jejich digitální zpracování nezbytný převod do číselné reprezentace pomoci analogově-digitálního převodníku (ADC). Po konverzi musí být proveden opačný proces, aby bylo možné signál zase spojit se zbytkem syntezátoru. Současně také vysvětluje koncepty vzorkování, kvantování a kódování. Nakonec je zde prozkoumán význam algoritmů se zaměřením na jejich implementaci pomocí digitálních signálových procesorů.

Cílem druhé části je navrhnout programovatelnou efektovou jednotku ve formě modulu Eurorack s vhodným ovládáním. K dosažení tohoto cíle je stanoven návrhový cíl, kde je uveden určitý počet ovládacích prvků a funkcí, které mají být implementovány. Vlastnosti a parametry FV-1 popisuji omezenou sadu možností, které lze implementovat: efektová jednotka může mít pouze tři parametry a pouze 8 uživatelských programů. Neexistuje také žádná paměť přednastavení. Kromě toho nejsou k dispozici žádné dedikované možnosti pro míchání zpracovaných a nezpracovaných signálů. K dosažení těchto funkcí by bylo nutné obětovat některé kontrolní parametry. K překonání těchto omezení, je využit mikrokontroler Raspberry Pi Pico. Toto rozšíření umožnilo také využít displej pro zobrazení názvů efektů a parametrů. Jednotka mikrokontroleru je také použita k sériovému zápisu nových programů do EEPROM, ke kterému je FV-1 připojen. Tím je realizován programovatelný aspekt tohoto efektového modulu. FV-1 a Pico jsou navíc vzájemně propojeny v dalších klíčových aspektech. Piny pro výběr programu u FV-1 jsou přímo připojeny k Pico,

což umožňuje Pico určovat, který efekt je aktuálně načten do paměti FV-1. DSP parametry FV-1 jsou obdobně ovládány Pico. K dosažení těchto cílů jsou řídicí napětí nejprve přečtena ADC Pico a poté je použito PWM spolu s dolní propustí.

Také je navržena analogová periferie pro úpravu hlasitosti a obvod pro míchání zpracovaného a nezpracovaného signálu. Po popisu celkové architektury je každý z komponentů vysvětlen podrobněji. Pro každý obvod jsou vypočítány hodnoty součástek a pokud jsou dostupné modely, obvody jsou testovány pomocí počítačové simulace.

Následně byla vyvinuta deska plošných spojů (PCB) společně s panelem a také je zde popsán kód napsaný pro mikrokontroler.

KLÍČOVÁ SLOVA

Modulární syntezátor, Eurorack, Digitalní efekt, Číslicové Zpracování Signálů, DSP, mikroprocessor

Author's Declaration

Author:	Bc. Pavlo Shelemba
Author's ID:	212579
Paper type:	Bachelor's Thesis
Academic year:	2022/23
Topic:	Programmable Digital Multi-Effect

I declare that I have written this paper independently, under the guidance of the advisor and using exclusively the technical references and other sources of information cited in the paper and listed in the comprehensive bibliography at the end of the paper.

As the author, I furthermore declare that, with respect to the creation of this paper, I have not infringed any copyright or violated anyone's personal and/or ownership rights. In this context, I am fully aware of the consequences of breaking Regulation § 11 of the Copyright Act No. 121/2000 Coll. of the Czech Republic, as amended, and of any breach of rights related to intellectual property or introduced within amendments to relevant Acts such as the Intellectual Property Act or the Criminal Code, Act No. 40/2009 Coll. of the Czech Republic, Section 2, Head VI, Part 4.

Brno ....

author's signature*

*The author signs only in the printed version.

ACKNOWLEDGEMENT

I would like to thank the advisor of this work, Ing. David Kubánek, Ph.D., for his invaluable insights and suggestions. My deepest gratitude goes to Martin Kecl, Václav Mach and all the beautiful people of *Bastl Instruments*, without whom this work would not be possible. I would also like to express my sincere gratitude to Kim Bjørn of Bjooks for their permission to adapt the patch symbols from their book *PATCH & TWEAK*.

Contents

List of Figures

List of Tables

Introduction

This work is devoted to the study of Digital Signal Processing (DSP) and its implementation in the embedded context. In particular, a specific digital signal processor was chosen to build an Eurorack synthesizer module, the Spin Semiconductor FV-1.

The work is divided into two parts. First, it discusses the theoretical foundations necessary to successfully design a modular synthesizer. Starting from the concept of sound itself, it goes over the basic building blocks of sound synthesis. It explains the importance of voltage control, and how it enables interactions in the modular synthesizer. It analyzes common synthesizer building blocks in terms of four fundamental components: audio sources, audio modifiers, modulation sources and modulation modifiers. It then explains how these concepts are translated into the world of modular synthesis. Then, the details of the Eurorack modular synthesizer format are explained. For this, its mechanical and electrical specifications are listed. Then, it goes over the fundamentals of the DSP. It explains the importance of digital signal representation, and goes over the fundamentals of digitizing the sound. For this, it explains the concepts of sampling, quantization a coding. Finally, the importance of algorithms is explored, with a focus on their implementation using the digital signal processors.

The aim of the second part is to design a programmable multi-effect unit in the form of an Eurorack module with appropriate user control. To achieve this, a design goal is set, where a specified number of user controls and functions to be implemented is listed. The properties and parameters of the FV-1 dictate a very restricted set of controls and options to be implemented: the effect unit may have up to three parameters and only up to 8 user programs. There is also no preset memory. Additionally, there are no dedicated options for bypassing or mixing processed and unprocessed signals together. To achieve these functions, some control parameters and processing cycles would have to be sacrificed. To circumvent such limitations, a microcontroller unit is introduced, along with the analog peripheral circuitry, like volume control and Dry/Wet mixing circuit. After the discussion of the overall architecture, each of the components is explained in greater detail. Component values for each circuit are calculated, and when the models are available, the circuits are tested using a computer simulation. The printed circuit board (PCB) and the panel are developed. The code written for the microcontroller is subsequently discussed.

1 Theory

This chapter discusses the theoretical foundations necessary for the successful design of modular synthesizers. It goes over basic ideas commonly used in the field of sound creation and manipulation, starting from the concept of sound itself. It then explains the basic building blocks of sound synthesis, how they are usually connected, and how these conventions are translated into the world of modular systems. Then it provides standard parameters of the Eurorack modular synthesizer. Finally, it discusses the fundamentals of the digital signal processing and how it's implemented using digital signal processors.

1.1 Preliminaries

To design an effect unit with an adjustable level of processed and unprocessed signals, it's beneficial to start the discussion with the fundamental concepts of sound and how it's perceived by humans. Furthermore, to fully appreciate the intent behind certain elements of the modular system, it's similarly useful to discuss the basic ideas of voltage control and sound synthesis.

1.1.1 Physics of sound

Fundamentally, *sound* is a disturbance in the medium through which it propagates. Usually, this medium is air, where periodic changes in pressure give rise to perturbations. Such periodic motion is generally described as a *wave*. [1]

Sound waves

Sound waves travel through the medium by displacing differences in pressure. As they propagate, wave particles oscillate around the point of zero displacement. When describing waves, it's useful to think of such simple harmonic motions, as we can use them to describe wave propagation, string vibrations of an instrument, or vibrations of the basilar membrane which converts acoustic energy into nerve pulses within our ear.

Displacement of simple harmonic motion relates to time as

$$y(t) = y_{\mathrm{m}} \sin\theta = A \sin(\omega t + \phi_0), \tag{1.1}$$

where y_{m} is the amplitude of the motion, θ is angular displacement, ω is angular velocity, t is time and ϕ_0 is the initial phase. Angular velocity relates to the rate of change, or frequency f, as $\omega = 2\pi f$.

By projecting simple harmonic motion through time, we get a sinusoidal motion, which can be described in terms of amplitude, frequency, intensity, and speed. [1]

Wave properties

The *amplitude* of a wave is the distance between maximum displacement and equilibrium. For sound waves, it's a distance between maximum or minimum pressure and standard atmospheric pressure, and it is often measured as average pressure variation per unit area or *Sound Pressure Level* (SPL).

The strength of pressure fluctuations is described as intensity. *Intensity* I describes power P flowing per unit area a as

$$I = \frac{P}{a^2} = \frac{E/t}{a^2} \; [\mathrm{W/m^2}], \tag{1.2}$$

where E/t is the energy E of wave motion per unit of time t, that flows into the ear and is perceived as sound.

Often it is easier and more useful to measure sound pressure instead of intensity. Intensity I is proportional to the square of the pressure change Δp as

$$I = \frac{\Delta p^2}{V\delta} \; [\mathrm{W/m^2}], \tag{1.3}$$

where V is the velocity of sound in air, δ is the density of air.

To measure quantities that can span a vast range of values, such as pressure, intensity or voltage, the logarithmic decibel scale is commonly employed. Using equation 1.3, we can calculate SPL as

$$L_\mathrm{p} = 10\log_{10}\left(\frac{I}{I_\mathrm{ref}}\right) = 10\log_{10}\left(\frac{p^2}{p_\mathrm{ref}^2}\right) = 20\log_{10}\left(\frac{p}{p_\mathrm{ref}}\right) \; [\mathrm{dB}], \tag{1.4}$$

where p is the *root-mean-square* (RMS) value of the sound pressure and p_ref is a reference sound pressure. [1]

1.1.2 Perception of sound

The human *hearing range* describes the perceptible frequency bandwidth of a sound, and can depend on many aspects, like physiology and age. It's usually said to span from 20 Hz to 20 kHz, although a 16 Hz to 16 kHz range is also cited.

Perceived *loudness* of a sound is closely related to the soundwave intensity. Our perception of sound intensity is limited by the threshold and limit of hearing. The *threshold of hearing* is the minimum sound intensity required to be detected, while the *limit of hearing* sound intensity is potentially painful. For 1 kHz, sound intensity at the threshold of hearing is approximately $t_\mathrm{h} = 10^{-12}\,\mathrm{W/m^2}$, while the limit of hearing is $l_\mathrm{h} = 10^{0}\,\mathrm{W/m^2}$.

Besides intensity, loudness is influenced by the range and complexity of sound's harmonic content. For example, our ear is less sensitive to very low and very high frequencies, but is more sensitive to the range of 1–3.5 kHz, so we perceive tones of these frequencies as louder compared to other tones of equal intensity. This is demonstrated in figure 1.1, which illustrates the equal loudness contours, as defined by the phon scale. [1]

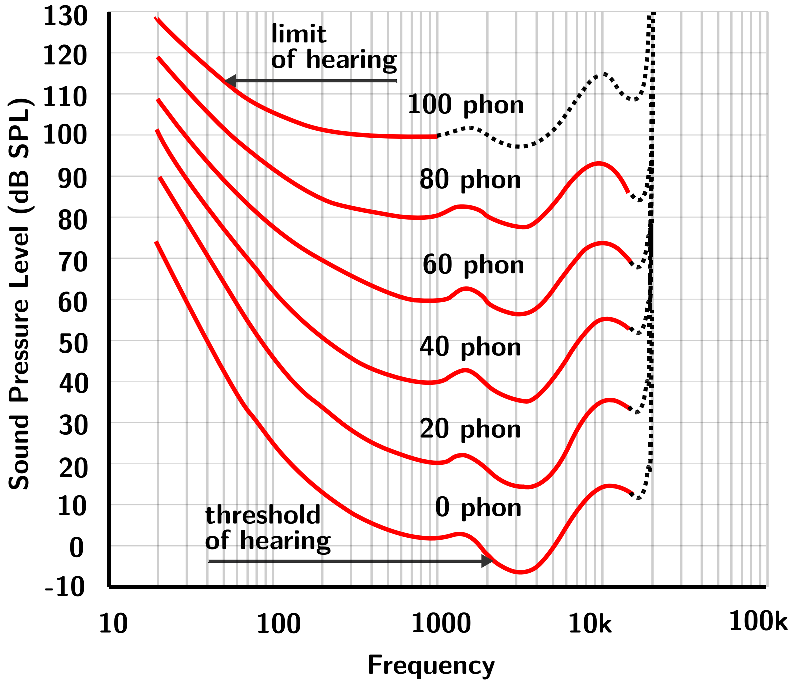

Fig. 1.1: Equal loudness contours [1]

1.1.3 Electronic sound synthesis

A *synthesizer* is an electronic instrument designed to generate audible voltage fluctuations. While numerous techniques exist to achieve this phenomenon, most synthesizers can essentially be distilled down into four fundamental components:

- Audio sources;
- Audio modifiers;
- Modulation sources;
- Modulation modifiers.

The following section explores these components in more detail and demonstrates two popular (but not exclusive) approaches to their interconnection. To illustrate these concepts, a common set of patch symbols has been used. These symbols originate from the book *PATCH & TWEAK* by Kim Bjørn and Chris Meyer, published by Bjooks, and are licensed under CC BY-ND 4.0. Permission to adapt certain symbols for this thesis was generously granted by the authors. [2]

Voltage control

Although all analog synthesizer signals are essentially variable voltages, they are usually divided into several categories based on their function:

1. Audio signals
2. Control voltages (CV)
3. Pitch voltages
4. Trigger, Gate, and Clock signals

Audio signals are produced by the audio sources and audio modifiers and can be perceived by the human hearing.

Control voltages are produced by the modulation sources and modulation modifiers and are used to modulate certain parameters of synthesizer sources and modifiers. These are usually below hearing range. Figure 1.2 demonstrates the principle of voltage control, where the filter cutoff frequency is being modulated by the fluctuating voltage.

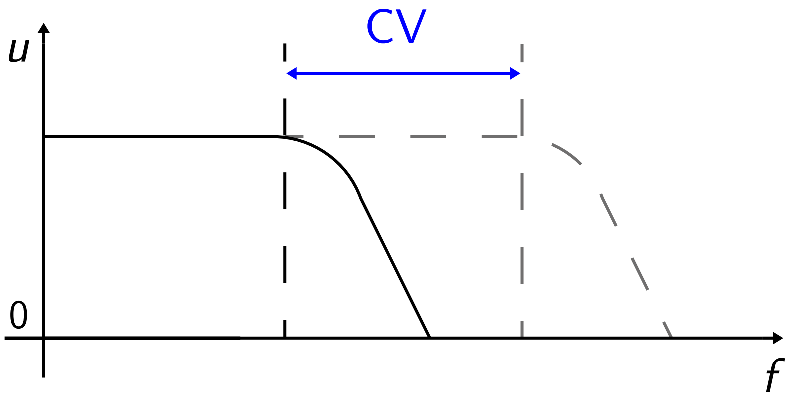

Fig. 1.2: Example of a filter cutoff modulation [2]

Pitch voltages are a special kind of CV that are used to define the rate of oscillation of certain audio sources. Several voltage to pitch standards exist, but the most popular one defines a change in one volt as a pitch change of one octave. Such pitch inputs are usually revered to as 1 V/oct.

Trigger, Gate, and *Clock signals* are other special kinds of CV, which initiate events, define their lengths and indicate event timing respectively. They are typically generated as pulse-shaped signals, where modules respond to their rising edge. Figure 1.3 shows an example of a gate signal triggering an envelope generator to produce its predefined voltage shape.

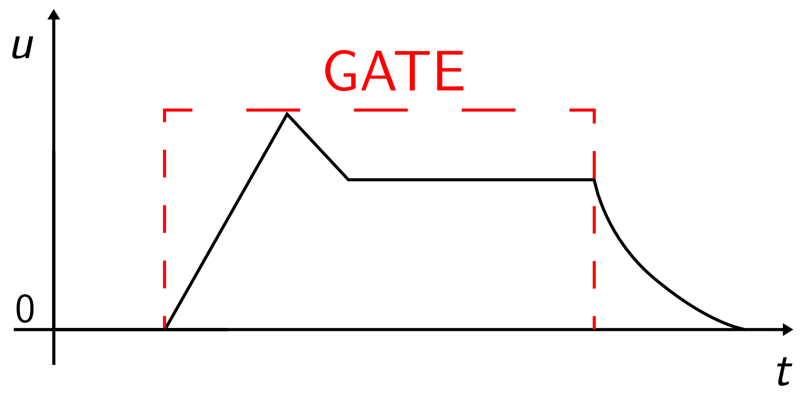

Fig. 1.3: Example of the envelope triggering [2]

It's worth noting, that even though in a context of a traditional synthesizer architecture such definitions are appropriate, in a modular system all modules produce the same analog voltages, and as such can be used as audio signals or control voltages. For example, a low frequency oscillator (LFO) may be used as an audio signal, a CV for an amplifier, or as a clock for a sequencer. Similarly, audio signals may be used for audio-rate modulation of many synthesizer parameters. [2]

Audio sources

At the core of a typical electronic synthesizer architecture is a *tone generator*. Most commonly, it's represented by an *oscillator*, which can generate voltages fluctuations within the audible range. Figure 1.4 shows symbols for some of the more common tone generators, which are discussed below.

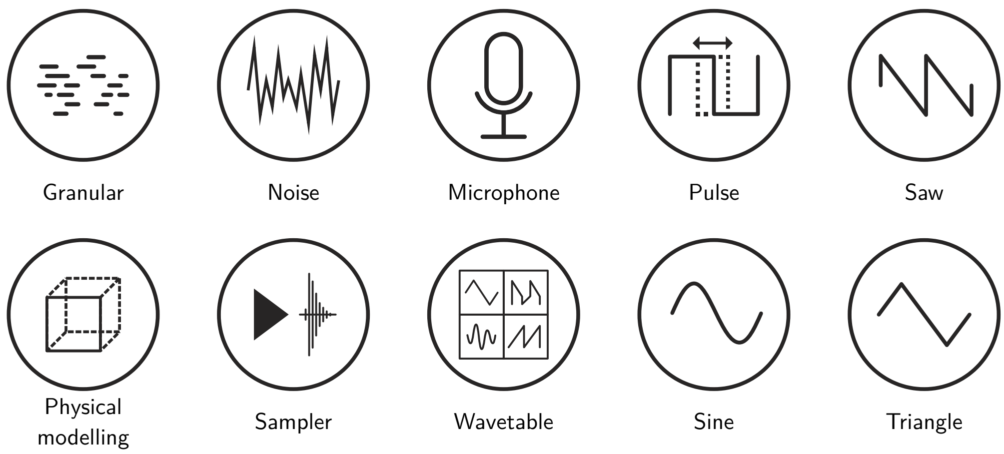

Fig. 1.4: Common tone generators [2]

Traditional voltage oscillators can generate a set of predefined waveshapes:

- *Sine wave* contains only the fundamental frequency;

- *Square wave* contains only odd harmonics;
- *Pulse wave* is a square wave with a variable duty cycle;
- *Triangle wave* contains only odd harmonics, but higher ones roll off much faster than in a square wave;
- *Sawtooth wave* contains both even and odd harmonics.

More recent oscillator architectures are often digital in nature and allow for much more flexible tone generation. These may include:

- *FM oscillators* employ frequency modulation of one tone generator by another one;
- *Wavetable oscillators* store the desired waveshape in memory as a series of numeric values;
- *Physical modelling oscillators* generate sounds based on the mathematical model of a real instrument;
- *Virtual analog oscillators* recreate stochastic characteristics of analog circuits;
- *Samplers* allow playback of digital recordings;
- *Granular oscillators* special kinds of samplers, which play tiny pieces of sound at variable positions of the original sample;
- *Macro oscillators* contain numerous kind of oscillators, which can be easily switched.

Another common tone generator is the noise source. It's usually referred to by the color, which describes its frequency spectrum energy distribution:

- *White noise* has equal power in every linear band of frequencies;
- *Pink noise* has equal power in every logarithmic band of frequencies, so power reduces by 3 dB for each subsequent octave;
- *Brown noise* has power reduced by 6 dB for each subsequent octave;
- *Blue noise* has power increased by 3 dB for each subsequent octave;
- *Purple noise* has power increased by 6 dB for each subsequent octave;
- *Grey noise* has power adjusted for the loudness curve.

Such noise is usually generated using analog components. Digital noise sources, of course, exist and may have additional qualities not defined by the standard color scheme, such as grittiness or harmonic components. [2]

Audio modifiers

Audio modifiers serve to alter generated audio signals. Some common modification methods include the addition or removal of harmonics, temporal control of loudness, signal mixing and routing, and the application of various effects. Figure 1.5 illustrates several frequently used modifiers, some of which will be discussed below.

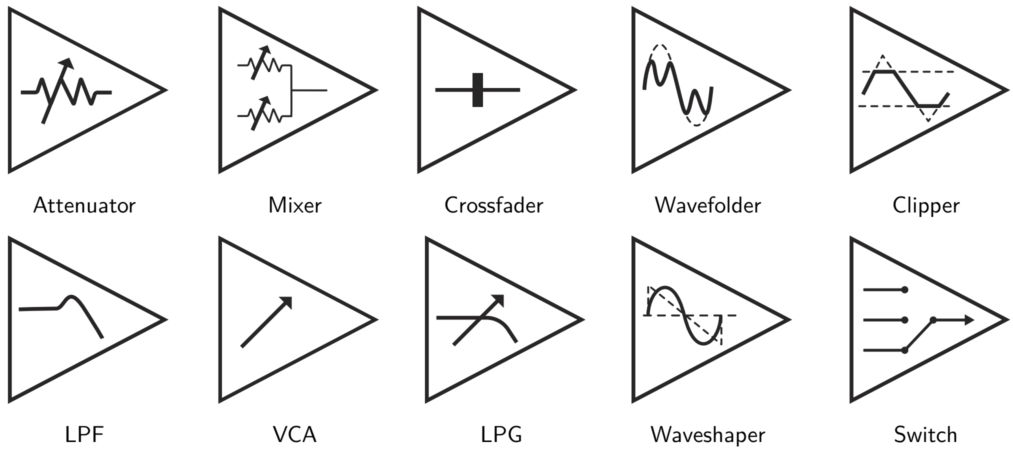

Fig. 1.5: Common audio modifiers [2]

A *voltage-controlled filter* (VCF) can be employed to enhance or suppress specific harmonics:

- A *Low-pass filter* (LPF) permits harmonics below a specified cutoff frequency.
- A *High-pass filter* (HPF) permits harmonics above a specified cutoff frequency.
- A *Band-pass filter* (BPF) permits harmonics at a particular cutoff frequency.
- A *Notch filter* (N) suppresses harmonics at a particular cutoff frequency.

To introduce additional harmonics, various types of *wave shapers* can be utilized:

- *Clipping, distortion*, and *saturation* limit the signal at the upper and lower boundaries of the waveform;
- *Full-wave rectifiers* invert the lower portion of the waveform;
- *Half-wave rectifiers* eliminate the lower portion of the waveform;
- *Wavefolders* fold the waveform onto itself;
- *Waveshapers* bend the waveform into different shapes.

To modify the loudness of a signal, a variety of circuit types have been developed:

- An *attenuator* allows for passive regulation of the signal level;
- A *mixer* consists of multiple attenuator inputs that allow to combine signals together;
- A *crossfader* is a dual attenuator that inversely modifies the levels of two connected signals;
- A *voltage-controlled amplifier* (VCA) can be manipulated using CV to regulate the signal level over time;
- A *switch* can be used to control which signals appear on the output.

A *low-pass gate* (LPG) merges the concepts of a VCF and a VCA. With an increase in Control Voltage (CV), both the volume and the frequency bandwidth of the incoming signal increase. Conversely, a decrease in CV results in a corresponding decrease in the volume and frequency spectrum of the signal. [2]

Modulation sources

Modulation sources or modulators serve to generate CVs of various kinds. They generate variable voltages over time that are used to control the operation of other modules. Some sources are shown in figure 1.6 and are discussed below.

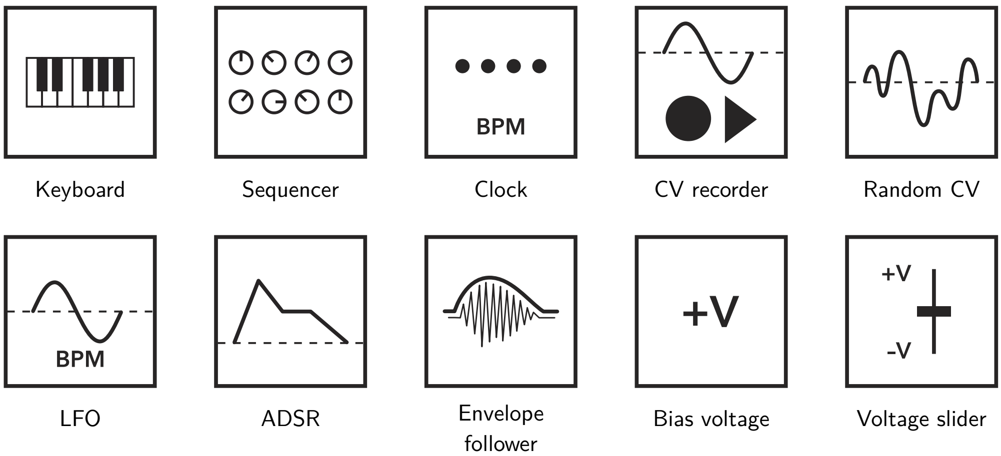

Fig. 1.6: Modulation sources [2]

Modulators can be divided into four categories:

- Envelope generators
- Low frequency oscillators
- Random sources
- Controllers

Envelope generators (EG) create multistaged voltages, which first rise to the maximum value, and then descend according to the specified shape. They are usually initiated by a gate or a trigger and are commonly used to control audio modifiers like VCF and VCA. It's also possible to generate the envelope from the incoming signal itself using an *envelope follower*.

Low frequency oscillators (LFO) usually generate cyclical voltages below the hearing range.

Random sources work similarly to the noise generators, but at a much slower rate. Generated voltages may be quantized or smoothed.

Controllers may be used to insert musical phrases, or provide possibilities for additional control over the parameters. These may include:

- Keyboard controllers
- Sequencers
- Touch strips

- Sliders, potentiometers, wheels
- Light and proximity sensors

Modulation modifiers

Modulation modifiers serve to process voltages generated by the modulation sources. Many of them mirror principles described in the audio modifiers section above, like mixers, attenuators and waveshapers. Some of the more commonly used CV modifiers are shown in figure 1.7.

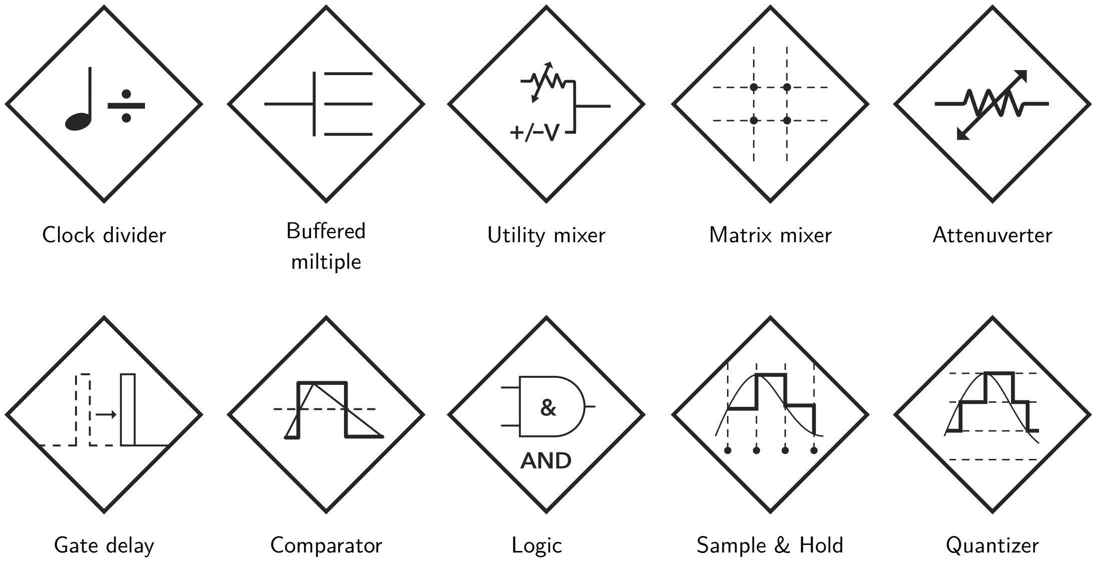

Fig. 1.7: Modulation modifiers [2]

1.1.4 Model synthesizer patches

While numerous approaches to synthesizer design have emerged through the years, the two most famous techniques have formed early on. Some American synthesizer companies from the east, like Moog and ARP, were proponents of the *subtractive synthesis*, while some western US companies, like Serge and Buchla, often employed *additive synthesis* in their designs. [2]

East Coast patch

East Coast patches are characterized by the subtractive synthesis approach, where a harmonically rich audio source is being processed by the audio modifiers like VCF and VCA. Therefore, a common goal of such patches is to remove or highlight certain harmonics.

Figure 1.8 shows a basic example of the subtractive patch. The yellow arrow represents the audio signal. When the key of the keyboard controller is pressed, multiple types of CVs may be generated. The gray arrow represents pitch CV, which is connected to the VCO and controls the frequency of its oscillations. The red arrow represents the gate CV, which triggers the envelope. The envelope generates multistaged CV (blue arrows), that modulate the filter and amplifier parameters.

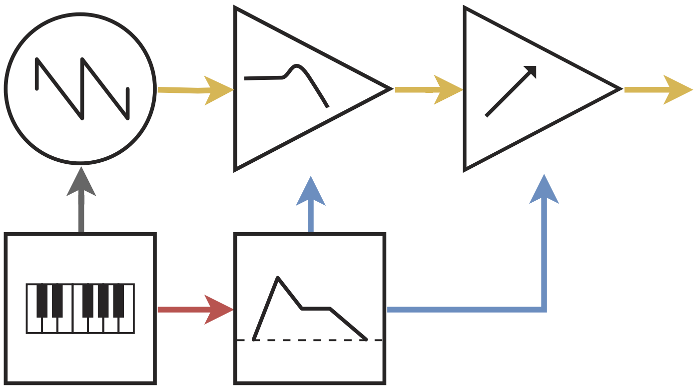

Fig. 1.8: Basic East Coast patch [2]

West Coast patch

West Coast patches are characterized by the additive synthesis approach, where a harmonically simple audio source is being processed by the audio modifiers like wavefolder and LPG. Thus, the common goal of such patches is to add harmonics.

Figure 1.9 shows a basic example of the additive patch. The voltage sequencer generates pitch and gate CVs to control a sine oscillator and an envelope, respectively. The sine oscillator is being shaped by the waveshaper, adding additional harmonic content. LPG allows to further sculpt the sound, both harmonically and temporally.

1.2 Modular synthesis

While typical synthesizer patches discussed in section 1.1.4 provide immense sound design possibilities, they are nevertheless limited by the predetermined connections between the components. The idea of the *modular synthesizer* is then to provide the ability to freely interconnect any sources with any modifiers using patch cables. [2]

This section will briefly mention common implementations of this idea, while mostly focusing on the specifics of the most popular modular format, the *Eurorack*.

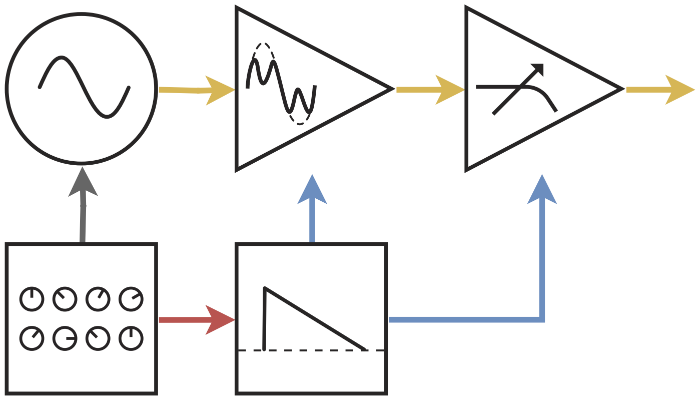

Fig. 1.9: Basic West Coast patch [2]

1.2.1 Formats

Over the history of electronic sound synthesis, several modular synthesizer formats have emerged. While there are various differences in design philosophies between them, the easiest way to discern them would be by their *height*:

3U: Eurorack

4U: Serge

4U: Buchla

5U: Moog,

where U stands for *rack units* and describes a standard rack spacing. 1U is 1.75 inches or 44.45 mm, and all the units are a multiple of this value. [2]

1.2.2 Eurorack specifications

The *Eurorack modular synthesizer* was originally conceived as the Doepfer Musikelektronik A-100 modular system in 1994. It's still offered as separate modules and in several pre-built configurations, one of which is shown in figure 1.10.

Mechanical details

The mechanical specifications of the Eurorack are based on the international standard 19-inch rack enclosure, as outlined by DIN 41494, IEC 297-3 and IEEE 1001.1.

Module front panels are 3U or 133.4 mm high. However, the actual height of the front panel is usually 128.5 mm to account for the rack mounting rails. The width of the module is measured in HP or *horizontal pitch units*. 1 HP is 1/5 inches or 5.08 mm, and all panels widths should be the multiples of this value. That said, the actual width of the front panel is once again a little smaller to account for tolerances while mounting the module in the rack. As is the case with the A-100 system, the

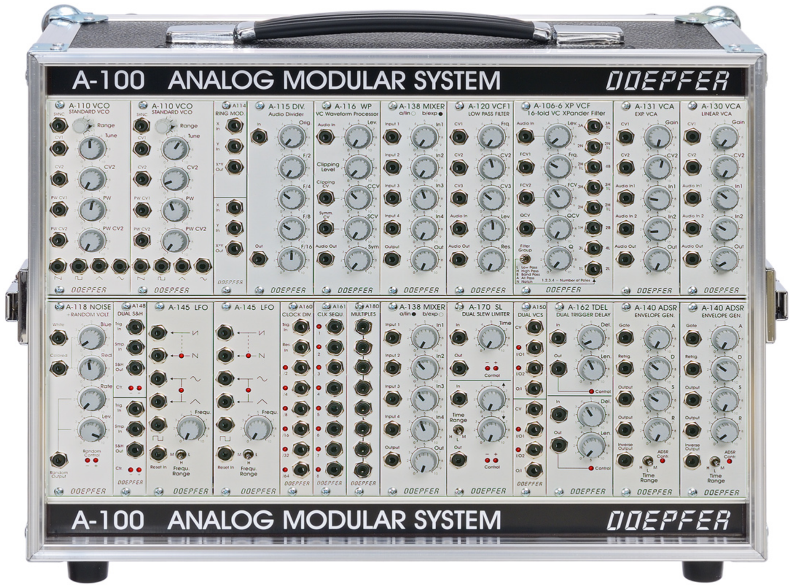

Fig. 1.10: Basic System 1 in portable 6U case A-100P6 [4]

front panels can be made of 2 mm anodized aluminum, but are also commonly found to be made of plastic, wood or even printed circuit boards (PCBs). All the unused space in the rack system should be covered up with blank panels due to safety and electromagnetic compatibility (EMC) reasons.

Figure 1.11 shows the main front panel measurements. For the front panels up to 10 HP, two mounting holes at the top and bottom of the panel are sufficient. Larger widths usually require four mounting holes. The horizontal distance of the mounting holes has to be a multiple of the HP grid. [3]

Patching is done via 3.5 mm Ring-Sleeve (RS) phone connectors, which are used for both audio and CV signals. [2]

Electrical details

Audio signals *typically* produce voltages from $-5\,\mathrm{V}$ to $+5\,\mathrm{V}$ ($10\,\mathrm{V_{pp}}$). However, real voltage ranges depend on the specific implementation and should be looked up in the manual. [3] This range is noticeably larger than the voltage ranges commonly found in consumer electronics ($\pm 0.45\,\mathrm{V}$ line level) and even professional sound equipment ($\pm 1.78\,\mathrm{V}$ line level), so they must be amplified by the appropriate input modules. [2]

Modulation signals are *typically* in a range from $-2.5\,\mathrm{V}$ to $+2.5\,\mathrm{V}$ ($5\,\mathrm{V_{pp}}$) for LFOs, and from $0\,\mathrm{V}$ to $+8\,\mathrm{V}$ for envelopes ($8\,\mathrm{V_{pp}}$). Again, real values may vary and should be checked with the manual.

Trigger, Gate, and Clock Signals have *typical* voltage levels from $0\,\mathrm{V}$ to $+5\,\mathrm{V}$ ($5\,\mathrm{V_{pp}}$), but can be as high as $+12\,\mathrm{V}$ and should also be checked with the manual.

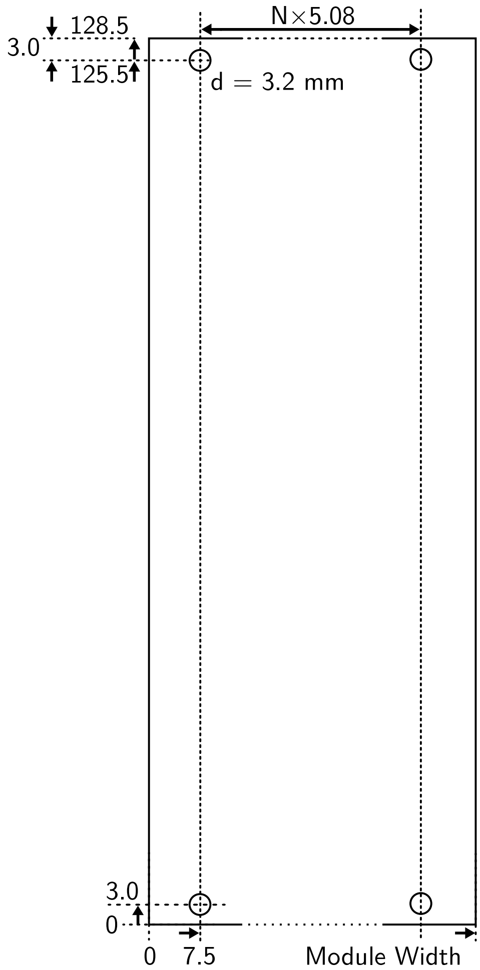

Fig. 1.11: A-100 front panel measurements [5]

Modules are supplied with power using a common bus board. It is expected that the power supply will generate at least +12 V and −12 V, but some modules may additionally require +5 V. As a rule, the −12 V is located on the bottom of the bus board, with an appropriate marking. The −12 V wire is typically marked red. [3]

Input impedance once again varies per module, but is usually expected to be around 100 kΩ. The same applies for output impedance, which is usually expected to be around 1 kΩ. [3]

1.3 Digital signal processing

This section discusses two fundamental concepts related to digital signal processing (DSP), *digital signals* and *digital systems*. [6]

1.3.1 Digital signals

As was stated in sections 1.1.3 and 1.2.2, Eurorack modular synthesizer works with analog voltages. Therefore, to apply DSP to such signals, they must be converted to a digital signal representation. After the conversion, a reverse process must be made for the signal to be interfaced with the rest of the synthesizer. Figure 1.12 demonstrates this process using an *analog-to-digital* (ADC) and *digital-to-analog* (DAC) converters.

Fig. 1.12: Digital processing of analog signals

To obtain a sequence of samples $x(n)$ that would correspond to the analog signal $x(t)$, a multistep process must be performed.

First, the amplitudes of $x(t)$ must be *sampled* at a constant rate, which is determined by the *sampling period* T, or more specifically by its inverse, the *sampling frequency* $f_\mathrm{S} = 1/T$. The sampling frequency indicates the sample count per second, measured in Hertz (Hz). Per sampling theorem, this frequency must at lest twice the frequency f_max of the analog signal $x(t)$: $f_\mathrm{S} > 2\,f_\mathrm{max}$. If the sampling frequency cannot be changed, the input signal must be within the bandwidth specified by $f_\mathrm{max} = f_\mathrm{S}/2$ to avoid undersampling and subsequent aliasing. *Aliasing* occurs when high-frequency components are incorrectly interpreted as lower-frequency components during the sampling process. To prevent this, a low-pass antialiasing filter is usually employed, which would permit frequencies up to f_max only. [6]

After signal amplitudes are captured for each sampled moment, their values are *quantized* to a grid of predetermined values according to the resolution of the ADC. For a 16-bit ADC, this would mean $2^{16} = 65536$ unique values, allowing for a dynamic range of 98.08 dB. For higher ranges, the difference between sampled and real values, or *quantization noise*, becomes problematic, and so a higher precision ADC would be required. [7]

The quantized amplitude values are then encoded into a digital signal $x(n)$, which is then routed to a digital signal processor, where a specified algorithm calculates an output sequence of numbers $y(n)$ based on the provided input sequence. This sequence is subsequently sent to a DAC, which reconverts it into the analog signal $y(t)$. [6]

1.3.2 Digital systems

A *digital system* is essentially a DSP algorithm which manipulates an incoming stream of numerical data x(n) with mathematical operations such as addition, multiplication, and time delay. The output of the algorithm is a new sequence of numerical data, the output signal y(n).

Two main processing methods are

- Block processing
- Sample-by-sample processing

In *block processing*, samples accumulate in a storage buffer and are only processed when the buffer is fully populated with new data. This method is exemplified in processes like Fast Fourier Transforms (FFTs) used for spectral analysis and rapid convolution operations.

Sample-by-sample processing handles each input sample individually as it arrives. [6]

1.3.3 Audio signal processors

Given the real-time requirements of *audio signal processors*, they typically employ sample-by-sample processing, where the same algorithm is applied to each incoming audio sample, to generate a corresponding output sample.

Audio signal processors store these samples and perform basic mathematical operations on them, such as addition, subtraction, and multiplication. These operations can involve constants or other sample values. Each processor has a unique *architecture*, which is a layout of processing elements that can execute these operations. For example, mathematical operations are usually carried out by the arithmetic unit, while the delay is implemented using a delay Random-Access Memory (RAM). Each architecture necessitates a distinct instruction set that aligns with its capabilities.

The processor executes a series of operations, which together define an algorithm. A set of these algorithms, in turn, constitutes a program. Developers write these programs in a human-readable assembly language that is specific to each processor. Each instruction in this language tells the processor to perform a particular operation and usually includes arguments that specify which memory elements or constants the operation should use. Typically, each line of a program represents a single instruction.

Once a program is complete, it is assembled from the human-readable program text into a compact sequence of control words. The processor stores these control words in the specified memory location and executes them in sequence during normal operation. [7]

2 Implementation

This chapter proposes a practical application of the theoretical concepts discussed in the previous chapter to construct a digital effects audio processor for an Eurorack modular synthesizer. It begins by outlining the overarching design objectives of the module. Following this, the most important electrical components are listed, as they shaped the specifics of the circuit and PCB design. These design specifics are then explored in detail. Finally, the software developed for the application is explained.

2.1 Design goals

The proposed synthesizer module is a programmable multi-effect audio processor based on the popular Spin Semiconductor FV-1 digital signal processor.

The module is designed to meet the Eurorack specifications, as described in section 1.2.2. The user-facing panel is 128.5 mm tall and 11 HP wide. The module requires $\pm 12\,\mathrm{V}$ for normal operation. All inputs and outputs are designed to operate with signals from $-5\,\mathrm{V}$ to $+5\,\mathrm{V}$.

The module features a full stereo signal path with an adjustable attenuation of the input, an analog manually and voltage-controllable crossfader, and 3 manually and voltage-controllable DSP parameters, which can also be saved to memory and recalled when the effect is activated. A list of effects is navigated using the display and the encoder.

The front panel of the module is shown in figure 2.1. The following panel components are highlighted with respective numbers:

1. The *L IN* and *R IN* jack inputs process the incoming audio signals and are associated with the respective attenuation slider *L*. The left input is normalled to the right one, allowing for the processing of monophonic signals.
2. The *L OUT* and *R OUT* jack outputs are the last points of the module's signal path. They can output both processed and unprocessed audio signals, depending on the position of the *DRY/WET* slider.
3. The *A*, *B* and *C* jack inputs process the incoming CV signals for DSP parameter control. They are associated with the respective voltage offset sliders *A*, *B* and *C*.
4. The *MIX* jack input processes the incoming CV signal for crossfading between processed and unprocessed signals on the *L OUT* and *R OUT* outputs. It is associated with the respective voltage offset slider *DRY/WET*.
5. The *Encoder* allows the user to navigate the list of effects. The currently selected effect is activated by pressing it.

6. The *OLED* screen displays the currently selected program name and its three parameters.
7. The *L* input level slider corresponds to the *L IN* and *R IN* inputs. It enables manual attenuation of the incoming audio signals.
8. The *A*, *B* and *C* slide potentiometers correspond to the respectively named CV inputs. They provide manual control over the 3 parameters of the currently selected program.
9. The *DRY/WET* slide potentiometer corresponds to the *MIX* jack input. It provides manual control over the crossfading between processed and unprocessed signals on the *L OUT* and *R OUT* outputs.
10. The *LED* monitors the input and output signal level of the module. If a signal level at the input or the output is too high for the processor, the LED flashes.

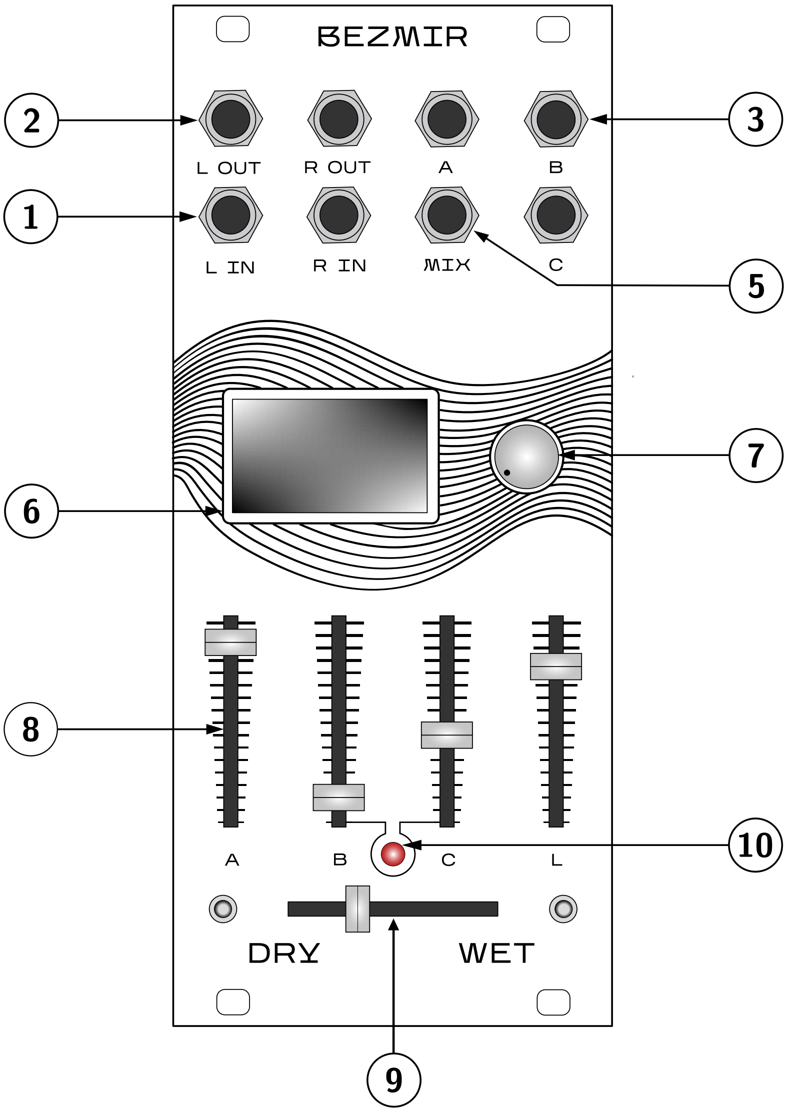

Fig. 2.1: Panel design of the proposed module

2.2 Component selection

This section discusses some of the more significant components used to implement the effects unit described in section 2.1. While the complete specifications can be found in the respective datasheets listed in the bibliography, some of the more relevant parameters are mentioned.

2.2.1 Digital signal processor

Shown in figure 2.2 is the *Spin Semiconductor FV-1*, a single-chip DSP solution designed specifically for audio effects applications. It integrates a 24-bit stereo ADC and DAC, which allows for straightforward connection of analog signals to and from the processor via simple coupling capacitors. Despite its digital nature, the FV-1 incorporates supply bypassing to minimize any radio frequency interference, and therefore can be safely inserted into the otherwise analog signal path. Its specifications are provided in table 2.1.

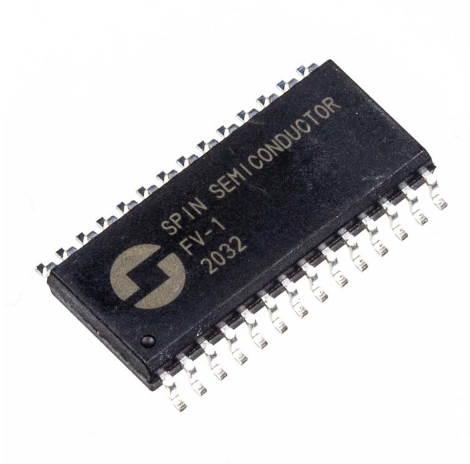

Fig. 2.2: Spin Semiconductor FV-1 [7]

The clock oscillator within the FV-1 can either accept an adjustable clock signal at the intended sample rate or function directly from an inexpensive watch crystal, which provides a sample rate of 32.768 kHz. In this case, signal bandwidth would be limited to roughly 15 kHz, which covers most of the perceptible audio range and is sufficient for most audio effects applications. This rate also enables full utilization of the FV-1's internal memory, providing up to one second of audio delay time.

The FV-1 also incorporates three potentiometer inputs that enable voltage controllable DSP parameters. These inputs are exposed as control parameters while programming the effect and may be used independently of each other. The potentiometer inputs are intentionally quantized to 9 bits with added hysteresis to prevent unwanted parameter fluctuations.

The FV-1 is a parallel processor, that can concurrently execute program instructions, manage memory addresses and generate sinusoidal and ramp LFOs. The provided instruction set is tailored for flexible audio effects programming, and includes many unique instructions. For instance, it has instructions for logarithm and exponent operations, which enable easily implementable dynamics processing and musical filtering. It also enables two-instruction filters (shelving HPF and LPF, allpass) that are particularly useful in reverb designs.

The FV-1 can access a total of sixteen programs, eight of which are built into the internal ROM, and another eight may be accessed through a serially connected EEPROM. To enable further expandability of available programs, a microprocessor can be utilized to dynamically write new programs to the EEPROM, as will be discussed in section 2.3.7. [7]

Tab. 2.1: Spin Semiconductor FV-1 specifications (clocked at 32.768 kHz) [8]

Analog supply voltage (AVDD)	3.3 V
Digital supply voltage (DVDD)	3.3 V
Positive reference (REFP)	3.3 V
Negative reference (REFN)	0 V
Operating temperature	0 °C to +70 °C
Analog input impedance	80 kΩ to 120 kΩ
Analog output impedance	50 Ω to 200 Ω
Allowable load resistance	10 kΩ
Maximum input signal level	2.6 V_{pp} to 3.0 V_{pp}
Maximum output signal level	2.6 V_{pp} to 3.0 V_{pp}
THD (1 kHz, −1 dB from clipping)	0.015 % to 0.03 %
ADC-DAC HF response (−3 dB)	14.5 kHz to 15.5 kHz
Total internal memory delay	1.0 s
Potentiometer control input impedance	10 MΩ to 20 MΩ
Supply current (AVDD + DVDD)	40 mA to 70 mA
REFP supply current	30 µA to 50 µmA
SDA and SCK internal pull-up	3.75 kΩ

2.2.2 Microcontroller unit

Even though a complete effects unit can be built using the FV-1 only, its design imposes certain restraints on the implementation, as was discussed in section 2.2.1. To allow for greater flexibility in the design, like an expanded selection of effects and the ability to display effect and parameter names on the screen, a *microcontroller unit* (MCU) has been introduced.

Shown in figure 2.3 is the *Raspberry Pi Pico*, a microcontroller board from Raspberry Pi. Built around the modern 40 nm RP2040 silicon, Pico combines low cost, high performance, and ease of use into a particularly flexible platform for embedded development. Its specifications are provided in table 2.2.

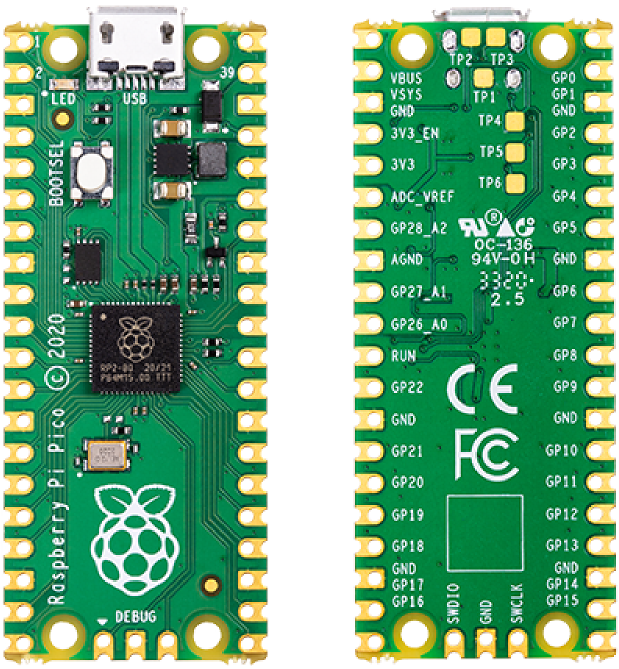

Fig. 2.3: Raspberry Pi Pico [9]

Pico provides the necessary minimum of external circuitry to operate the RP2040 chip: flash memory, crystal oscillator, power supplies and decoupling, and USB connector. Most of the RP2040 pins are available to the user through the I/O (Input/Output) pins on the left and right side of the board. Four of them are used for internal functions, such as driving an LED, power control and system voltage sensing. Pico uses an on-board buck-boost power supply to generate the required 3.3 V from a range of input voltages up to 5.5 V. Reprogramming the flash can be done using USB or the standard Serial Wire Debug (SWD) port. [9]

Tab. 2.2: Raspberry Pi Pico specifications [9]

Form factor	21 mm × 51 mm
CPU	Dual-core Arm Cortex-M0+ @ 133 MHz
Memory	264 kB multi-bank high performance SRAM 2 MB on-board QSPI flash with eXecute In Place (XIP) 16 kB on-chip cache
Interfacing	26 GPIO pins, including 3 analog inputs 3-pin ARM Serial Wire Debug (SWD) port 12-bit 500 ksps Analog to Digital Converter (ADC)
Peripherals	2 × UART 2 × SPI controllers 2 × I2C controllers 16 × PWM channels 1 × USB 1.1 controller (device and host) 8 × PIO state machines 1 × Timer with 4 alarms 1 × Real Time Counter
Input power	1.8 to 5.5 V DC
Operating temperature	−20 °C to +85 °C

2.2.3 Voltage controlled amplifiers

Voltage controlled amplifiers have been employed in several distinct parts of the circuit. Apart from attenuating input audio signals, they are an essential part of the crossfader implementation. All the VCAs in the circuit are the Sound Semiconductor SSI2164.

The SSI2164 is a flexible voltage controlled amplifier (VCA), suitable for high-performance audio applications. It features four separate gain cells that enable voltage regulation of current-mode inputs and outputs. The SSI2164 provides exponential control with a gain constant of $-33\,\mathrm{mV/dB}$, so for a full gain range of $+20\,\mathrm{dB}$ to $-100\,\mathrm{dB}$, control voltage should span from $-660\,\mathrm{mV}$ to $3.3\,\mathrm{V}$, respectively. In other words, attenuation of the incoming signal increases as the applied CV increases. It can be powered directly from the available $\pm 12\,\mathrm{V}$ [12]

2.2.4 Operational amplifiers

The proposed design uses two kinds of operational amplifiers (op-amps) for buffering, filtering, as well as voltage and transimpedance amplification and attenuation of the signals.

The audio signal path, as well as the crossfade circuit, make use of an industry-standard Texas Instruments TL072H. Although not exactly known for its high-performance audio characteristics, it remains a solid choice in cost-sensitive applications. TL072H can be powered directly from the available $\pm 12\,\mathrm{V}$ and features low offset voltage ($1\,\mathrm{mV}$, typical), high slew rate ($20\,\mathrm{V/\mu s}$), low offset voltage drift of $2\,\mathrm{\mu V/^\circ C}$, low power consumption ($940\,\mathrm{\mu A/ch}$, typical), low input bias and offset currents, low noise ($18\,\mathrm{nV}/\sqrt{\mathrm{Hz}}$ (typical) at $f = 1\,\mathrm{kHz}$), low total harmonic distortion ($0.003\,\%$), common-mode input to the positive supply, integrated EMI and RF filters and operation across the wide range of temperatures from $-40\,^\circ\mathrm{C}$ to $+125\,^\circ\mathrm{C}$. [10]

For the voltage-controllable DSP parameter inputs, a general purpose Microchip Technology MCP6002 was chosen. This op-amp operates from a single-supply voltage from $1.8\,\mathrm{V}$ to $6.0\,\mathrm{V}$, while typically drawing as low as $100\,\mathrm{\mu A}$ of quiescent current. The MCP6002 supports rail-to-rail input and output swing, with a common-mode input voltage range of $\mathrm{VDD} + 300\,\mathrm{mV}$ to $\mathrm{VSS} - 300\,\mathrm{mV}$, 90° phase margin (typical), and operation across the wide range of temperatures from $-40\,^\circ\mathrm{C}$ to $+125\,^\circ\mathrm{C}$. [11]

2.3 Schematic design

This section discusses the specifics of the module's electrical design. Figure 2.4 presents a basic outline of the proposed architecture.

As per the symbolic coding established in section 1.1.3, triangle symbols represent audio modifiers, thus the FV-1 uses this symbol. Diamond symbols, on the other hand, represent CV modifiers. Given that Pico processes incoming CV and generates corresponding voltages of its own, it uses this symbol.

As was described in section 1.1.4, the yellow arrows represent the audio signal path, while the blue arrows represent the control voltages. The names under the voltage sliders correspond to those on the user-facing panel. Audio and CV input and output jacks are marked with appropriate source symbols. The two names highlighted in blue indicate the specific type of waveshaping performed by the corresponding components.

The following section will describe each of the components shown in more detail. The entire schematic is presented in the appendix, where it was divided into the power (figure A.1), analog (figure A.2) and digital (figure A.3) sections.

2.3.1 Audio inputs

The module is designed to process both mono and stereo signals. This section focuses on the left input signal path. The right input is identical, with the only difference

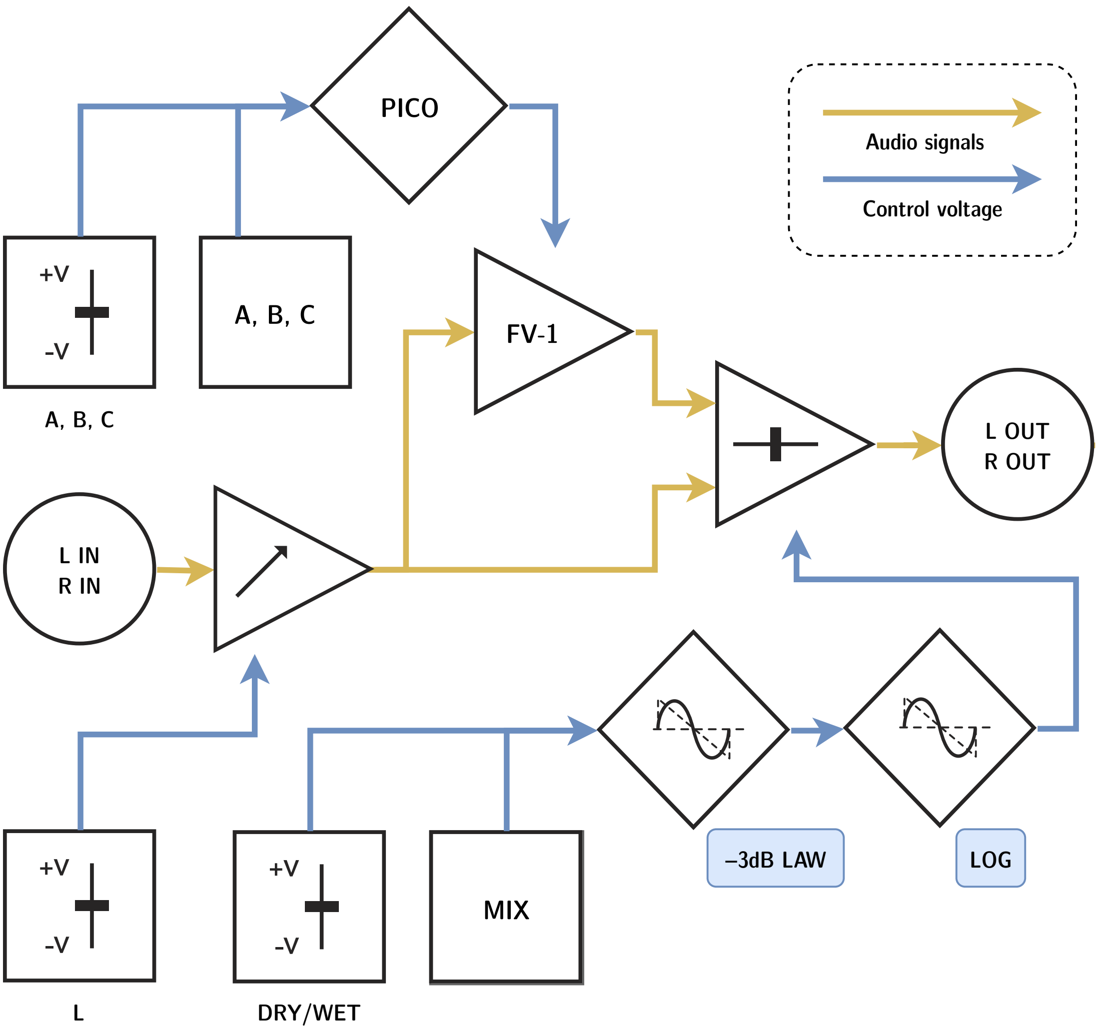

Fig. 2.4: Module architecture

being that the input is additionally normalized to the left input via the switch of the 3.5 mm jack socket. These inputs correspond to the *L IN* and *R IN* inputs on the panel.

Figure 2.5 shows a basic SSI2164 VCA circuit for one channel, as described in the datasheet [12]. An external amplifier, such as TL072H, is required to maintain the output current pin at a virtual ground. Together with a feedback resistor R_7, it serves as a transimpedance amplifier, converting the current output of the VCA into voltage. [12]

The audio input is designed to handle audio signals only, so a relatively large 10 µV electrolytic coupling capacitor is used. This capacitor is also recommended by the datasheet for improved control feedthrough. R_3 value of 100 kΩ was chosen to conform with the expected input impedance of an Eurorack module. This resistor converts the input voltage to current, and a 220 Ω resistor in series with a 1200 pF

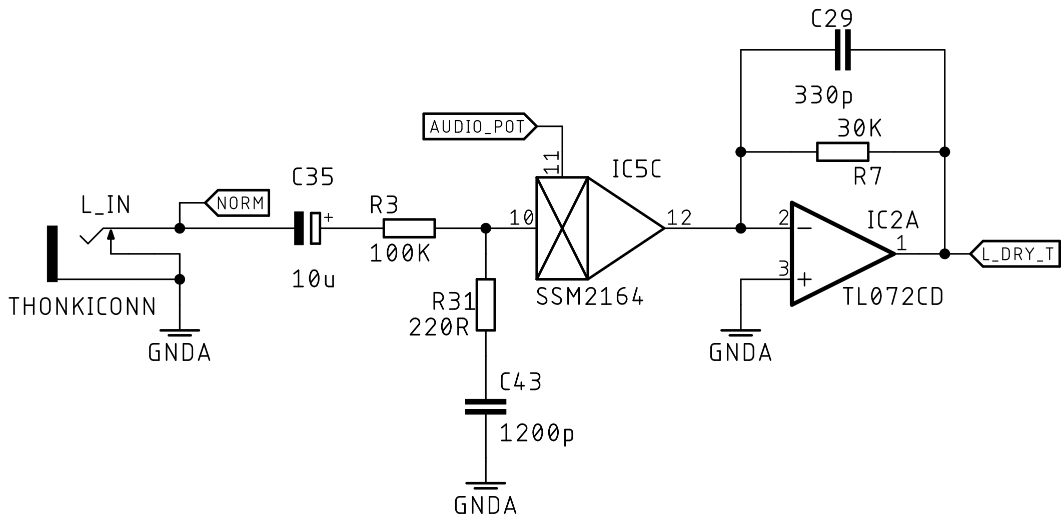

Fig. 2.5: Left input

capacitor connected to ground ensures stable operation of the VCA. [12]

According to the table 2.1, the maximum input voltage FV-1 expects to handle under normal operation is $3\,\mathrm{V_{pp}}$. Thus, the incoming $10\,\mathrm{V_{pp}}$ signal has to be attenuated to avoid damaging the FV-1. The closed-loop voltage gain of an inverting amplifier is given by

$$G = \frac{V_{\mathrm{out}}}{V_{\mathrm{in}}} = -\frac{R_{\mathrm{f}}}{R_{\mathrm{in}}} = -\frac{R_7}{R_3}, \tag{2.1}$$

where R_{f} is the feedback resistor and R_{in} is the input resistor. Thus, the value of the feedback resistor must be

$$R_7 = -R_3\,\frac{V_{\mathrm{out}}}{V_{\mathrm{in}}} = -100\,\mathrm{k\Omega}\cdot\frac{10\,\mathrm{V}}{3\,\mathrm{V}} = -30\,\mathrm{k\Omega}, \tag{2.2}$$

where the negative sign indicates inversion of the output signal with respect to the input. [13]

A feedback capacitor is used to preserve phase margin and minimize high-frequency noise often present in Eurorack synthesizer signal paths. [12] According to the table 2.1, for a clock frequency of $32.768\,\mathrm{kHz}$ the bandwidth of the FV-1 is around $15\,\mathrm{kHz}$ ($-3\,\mathrm{dB}$). To accommodate for this, the pole frequency f_{p} of the op-amp frequency response was set to $15\,\mathrm{kHz}$. Given that this frequency is given by [13]

$$f_{\mathrm{p}} = \frac{1}{2\pi\,C_{\mathrm{f}}\,R_{\mathrm{f}}}, \tag{2.3}$$

the required feedback capacitor value is

$$C_{\mathrm{f}} = C_{29} = \frac{1}{2\pi\,R_7\,f_{\mathrm{p}}} = \frac{1}{2\pi\cdot 30\,\mathrm{k\Omega}\cdot 15\,\mathrm{kHz}} = 353.68\,\mathrm{pF}. \tag{2.4}$$

The actual value was chosen as the closest E24 series value of 330 pF.

The circuit was simulated in LTSpice with a $10\,\mathrm{V_{pp}}$ $1\,\mathrm{kHz}$ sine signal, which corresponds to a VCO signal one may want to process with the module. VCA CV input was set to $0\,\mathrm{V}$ for a gain of $\mathrm{G} = 1$. The result of the simulation is shown in figure 2.6.

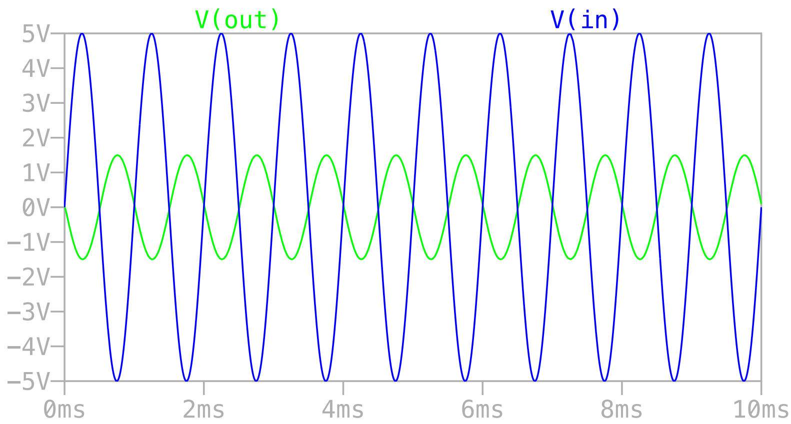

Fig. 2.6: LTSpice simulation of the audio input

CV for the VCA is generated using the audio taper slide potentiometer connected as a voltage divider, as shown in figure 2.7. This slider corresponds to the L input on the panel. The control input exhibits a standard impedance of $10\,\mathrm{k\Omega}$, so any resistance in series with the CV will cause slight attenuation of the control signal. Therefore, for a more accurate control of attenuation, CV is buffered using a Microchip MCP6002 op-amp in a unity gain configuration. [12] The rail-to-rail nature of this op-amp allows utilizing the full bandwidth of the VCA, while its large phase margin ensures its stability in the unity gain configuration. [11] With ensured low output impedance, CV is used for the simultaneous control of both left and right input VCAs.

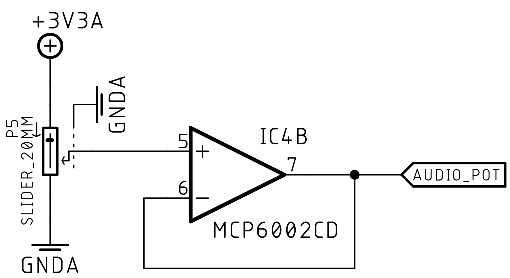

Fig. 2.7: Volume slider

From here, the audio signal is split into two independent signal paths, one of which is routed to the FV-1 and the other to the crossfade output circuit, both of which will be discussed in chapters 2.3.6 and 2.3.8.

2.3.2 Control voltage inputs

As discussed in section 2.2.1, FV-1 has three potentiometer inputs, which allow controlling three DSP parameters. To increase the design flexibility, these potentiometers are not connected directly to the IC. Instead, they are first sampled by the ADC of the Raspberry Pi Pico. Then, Pico's Pulse Width Modulation (PWM) is used to control the FV-1. The circuit is identical for all three control voltage inputs, so only one of them will be discussed in detail. These inputs correspond to the *A*, *B* and *C* inputs in the pannel.

Given that CV may have an intended offset, the input is DC coupled, meaning that there are no coupling capacitors on the inputs. As with the audio inputs, the expected CV input range is from −5 V to 5 V. Table 2.2 specifies that Pico operates at 3.3 V, so the incoming signals have to be attenuated. To achieve this, an inverting configuration of an MPC6002 op-amp is used, per application note [14]. Shown in figure 2.8, this circuit allows for the offset voltage adjustment while preserving an independent source resistance. The rail-to-rail nature of the MPC6002 and its single supply voltage of 3.3 V are used to limit the incoming voltage to the desired range from 0 V to 3.3 V. By using the negative reference voltage of −10 V, the output is offset by 1.65 V. A linear slide potentiometer serves as a voltage divider, allowing to control the offset manually. The default position of the potentiometer was chosen to be in the middle. This way, one may offset the input voltage both ways, allowing to adapt to various voltage ranges that may be present on the input.

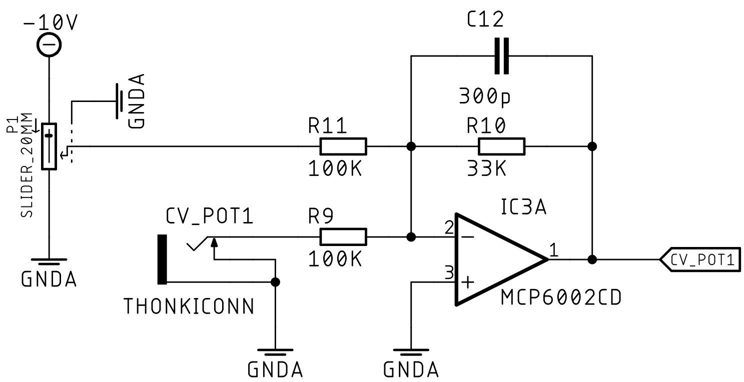

Fig. 2.8: Control voltage input with adjustable voltage offset

The output of the inverting op-amp can be derived from equation 2.1 as

$$V_{\text{out}} = -V_{\text{in}} \left(\frac{R_{\text{f}}}{R_{\text{in}}} \right) = -V_{\text{in}} \left(\frac{R_{10}}{R_9} \right). \tag{2.5}$$

To conform with the required input impedance of 100 kΩ, the value of R_9 was set accordingly. The value of the feedback resistor R_{10} is therefore

$$R_{10} = -R_9 \left(\frac{V_{\text{out}}}{V_{\text{in}}} \right) = -100\,\text{k}\Omega \cdot \left(\frac{3.3\,\text{V}}{10\,\text{V}} \right) = -33\,\text{k}\Omega. \tag{2.6}$$

For the default potentiometer position, the supply voltage V_S would be divided to $-5\,\text{V}$. In this configuration, when no signal is present on the input, the output should produce an offset voltage V_OS of 1.65 V. Therefore, the value of the offset input resistor R_{11} is

$$R_{11} = -R_{10} \left(\frac{V_\text{S}}{V_\text{OS}} \right) = -33\,\text{k}\Omega \cdot \left(\frac{-5\,\text{V}}{1.65\,\text{V}} \right) = 100\,\text{k}\Omega. \tag{2.7}$$

The feedback capacitor C_{12} is used to filter out the unwanted higher frequencies, that may be present in the input signal. As discussed in section 1.1.3, even though CVs are traditionally relatively low in frequency, nothing stops the user of the Eurorack modular system from sending audible range signals to these inputs. To accommodate for this, the pole frequency f_p of the op-amp frequency response was set to 16 kHz. As per equation 2.3, the required capacitor value is

$$C_{12} = \frac{1}{2\pi\, R_{10}\, f_\text{p}} = \frac{1}{2\pi \cdot 33\,\text{k}\Omega \cdot 16\,\text{kHz}} = 301.43\,\text{pF}. \tag{2.8}$$

The actual value was chosen as the closest E24 series value of 300 pF.

The circuit was simulated in LTSpice with a $10\,\text{V}_\text{pp}$ 10 Hz sine signal, which corresponds to an LFO signal one may use to control these inputs. The result of the simulation is shown in figure 2.9.

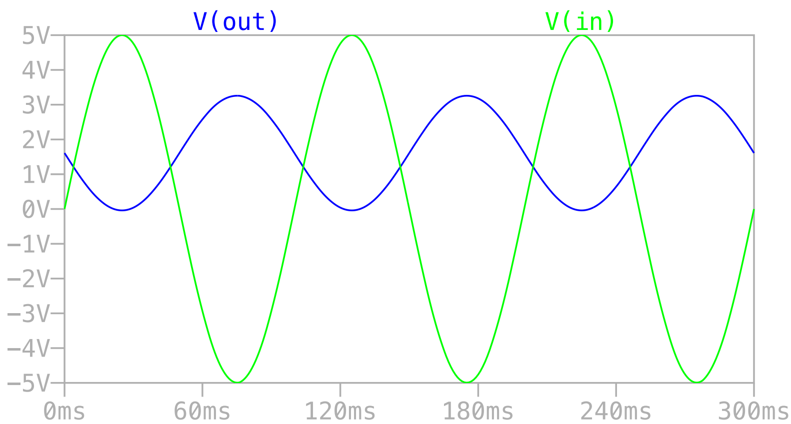

Fig. 2.9: LTSpice simulation of the CV input

2.3.3 Crossfade input

To enable voltage-controllable transitions between processed and unprocessed signals, a fully analog mixing signal path has been designed. This circuit is also based on the SSI2164 VCA, this time two gain cells per channel are used to control the volume of processed and unprocessed signals in tandem. The first stage of the cross-fader is the input, which works similarly to CV inputs discussed in section 2.3.2. The signal will be attenuated in the subsequent circuit, so there is no need for gain staging at this point. Instead, a TL072H op-amp serves as a unity gain buffer with an adjustable voltage offset, as shown in figure 2.10. The Jack socket corresponds to the *MIX* input, and the slider corresponds to the *DRY/WET* input on the panel.

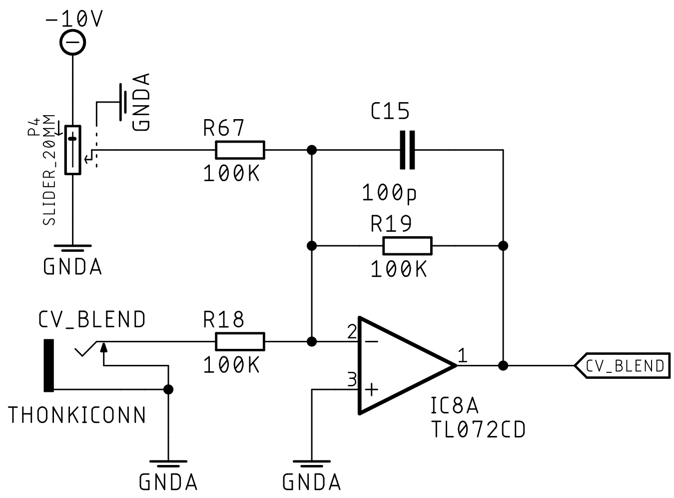

Fig. 2.10: Crossfade input with adjustable voltage offset

The unity gain buffer has the input impedance of $100\,\mathrm{k\Omega}$, set by the input resistor R_{18}. Therefore, the feedback resistor needs to be

$$R_{19} = -R_{18}\left(\frac{V_{\text{out}}}{V_{\text{in}}}\right) = -100\,\mathrm{k\Omega}\cdot\left(\frac{10\,\mathrm{V}}{10\,\mathrm{V}}\right) = -100\,\mathrm{k\Omega}. \tag{2.9}$$

As discussed in section 2.2.3, CV inputs of the SSI2164 VCA have a negative going gain constant of $-33\,\mathrm{mV/dB}$, so the input voltages must be offset to be of positive value only. Given the input voltage range from $-5\,\mathrm{V}$ to $5\,\mathrm{V}$, the offset voltage of $5\,\mathrm{V}$ is again designed for the middle position of the linear slide potentiometer, where the supply voltage V_{S} would be divided to $-5\,\mathrm{V}$. Therefore, the offset input resistor needs to be

$$R_{67} = -R_{19}\left(\frac{V_{\mathrm{S}}}{V_{\mathrm{OS}}}\right) = -100\,\mathrm{k\Omega}\cdot\left(\frac{-5\,\mathrm{V}}{5\,\mathrm{V}}\right) = 100\,\mathrm{k\Omega}. \tag{2.10}$$

The feedback capacitor C_{15} is once again used to filter out any unwanted higher frequencies above $16\,\mathrm{kHz}$, and is calculated as

$$C_{15} = \frac{1}{2\pi R_{19} f_{\mathrm{p}}} = \frac{1}{2\pi\cdot 100\,\mathrm{k\Omega}\cdot 16\,\mathrm{kHz}} = 99.47\,\mathrm{pF}. \tag{2.11}$$

The actual value was chosen as the closest E24 series value of 100 pF.

The circuit was simulated in LTSpice with a 10 V_{pp} 10 Hz ramp signal, which corresponds to an envelope signal one may use to control these inputs. The result of the simulation is shown in figure 2.11.

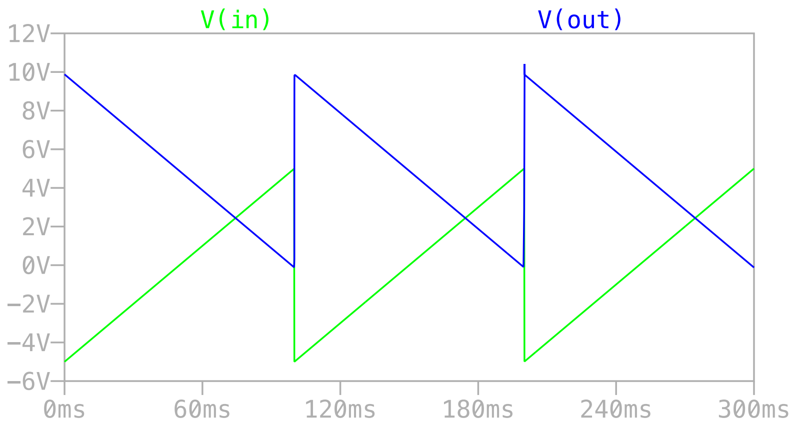

Fig. 2.11: LTSpice simulation of the crossfade input

To enable simultaneous volume control of both processed and unprocessed signals, another voltage with an opposite slope has to be generated. Shown in Figure 2.12, this circuit acts very similarly to the discussed input circuits, and only differs in the fixed voltage offset. Given the inverting configuration of this generator, the offset needs to be 10 V, hence the offset input resistor value of

$$R_{77} = -R_{37}\left(\frac{V_S}{V_{OS}}\right) = -100\,\mathrm{k\Omega}\cdot\left(\frac{-10\,\mathrm{V}}{10\,\mathrm{V}}\right) = 100\,\mathrm{k\Omega}. \tag{2.12}$$

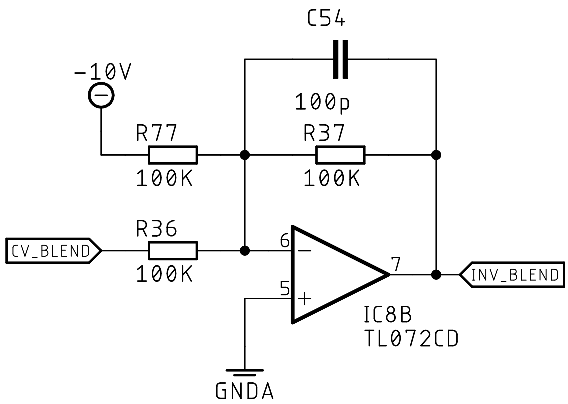

Fig. 2.12: Crossfade CV generator with the opposite slope

The circuit was simulated in LTSpice with an output from the crossfade input stage used as input voltage. The result of the simulation is shown in figure 2.13.

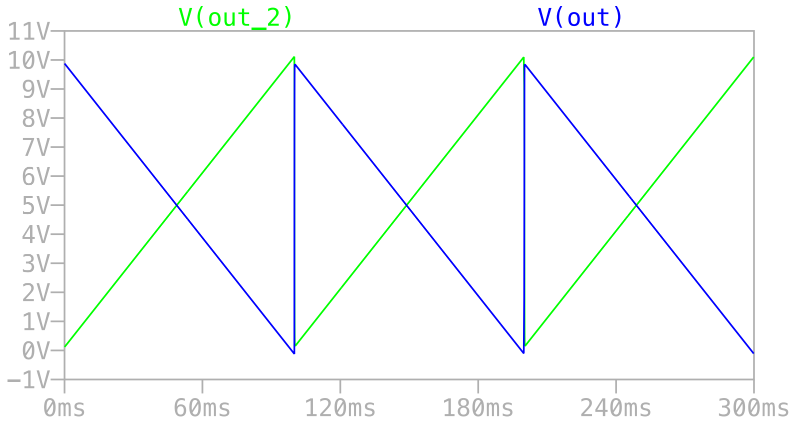

Fig. 2.13: LTSpice simulation of the reversed slope CV generator

2.3.4 Diode waveshaper

The input circuit of the crossfader provides two linear volume CVs that are inversely correlated. If these CVs were to be used for the attenuation of two signals with the same input amplitude, their gains would always sum to unity, or 0 dB. However, if we assume that the signals to be mixed are similar but non-coherent, as would be typical for this effects unit, the perceived loudness of the output signal would be affected. [15]

Per the discussion in section 1.1.1, the SPL in the center position of the transfer function is

$$L_p = 20\log\left(\frac{p}{p_{\text{ref}}}\right) = 20\log\left(\frac{0.5}{1}\right) = -6.02\,\text{dB}, \tag{2.13}$$

which can be observed in figures 2.13 and 2.14.

The sum of two non-coherent signals would therefore yield

$$\begin{aligned} L_\Sigma &= 10\log\left(\sum_{i=1}^{N} 10^{L_p/10}\right) = 10\log\left(10^{L_p/10} + 10^{L_p/10}\right) = 10\log\left(10^{L_p/10}\cdot 2\right) \\ &= 10\log 10^{L_p/10} + 10\log 2 = L_p + 3 = -3.02\,\text{dB}. \end{aligned} \tag{2.14}$$

To prevent this decrease in loudness, we can utilize the *constant power mixing* principle, also known as the -3 dB law, where curved CVs result in a 3 dB attenuation for the center position of the transfer function. Shown in figure 2.15, this arrangement ensures a constant-level summation for non-coherent signals.

One of the ways to shape the transfer function into the required curve is to use a piecewise linear approximation, where the approximated function is modelled by several linear segments with slopes or secants. Each slope intersects the modelled function at two points. In doing so, the effort is to ensure that the deviation of the approximation from the desired function does not exceed a certain limit, usually denoted as ε.

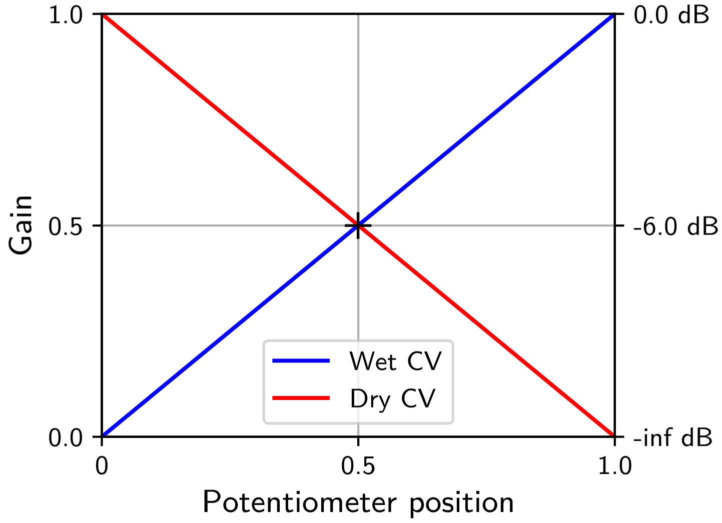

Fig. 2.14: Linear CV response

Figure 2.16 shows a diode waveshaper circuit that emulates a required nonlinear transfer function. Given the positive input signal and a negative reference voltage, the individual diodes will sequentially start conducting as the input voltage increases, thereby sculpting the transfer function in the intended way. [16]

The voltage gain of the op-amp can be described as a magnitude of the change of output voltage V_{out} relative to the input voltage V_{in}. The gain therefore indicates the slope of change

$$S = \frac{V_{\mathrm{out}}}{V_{\mathrm{in}}}. \tag{2.15}$$

This corresponds to how we would describe slopes of linear segments in piecewise interpolation:

$$s_n = \frac{\Delta y_n}{\Delta x_n} = \frac{y_n - y_{n-1}}{x_n - x_{n-1}}. \tag{2.16}$$

Therefore, piecewise interpolation can be realized by a gain-controlled amplifier. The goal is to design a circuit which would dynamically change the gain of the amplifier at the required break points of the interpolation. The first segment would have the smallest slope, which means that the gain of the op-amp should also be the lowest. As we gradually decrease the input resistance by connecting additional resistors in parallel to it, the gain and therefore the slope will increase.

To obtain the required resistor values, we need to normalize the break points of the interpolated function to the actual voltages:

$$\begin{aligned} U_{\mathrm{in},\,n} &= X_n = x_n\, U_{\mathrm{in,\ max}}, \\ U_{\mathrm{out},\,n} &= Y_n = y_n\, U_{\mathrm{out,\ max}} \end{aligned} \tag{2.17}$$

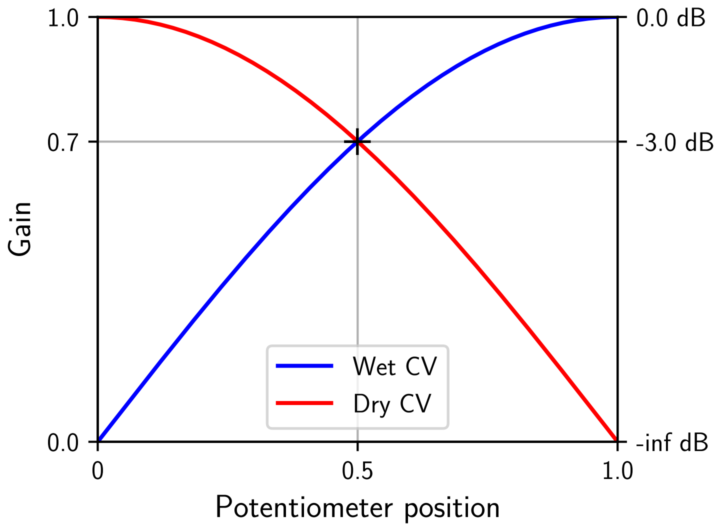

Fig. 2.15: Constant power CV response

Using values obtained from equation (2.17), we can calculate the voltage slopes of the circuit for each linear segment:

$$S_n = \frac{\Delta Y_n}{\Delta X_n} = \frac{Y_n - Y_{n-1}}{X_n - X_{n-1}}. \tag{2.18}$$

By deriving from equations (2.1) and (2.15), we can calculate the required values of resistances to be connected to R_{in} in parallel:

$$R_n = \frac{R_{\text{f}}}{|S_n - S_{n-1}|}. \tag{2.19}$$

The resistances calculated in equation (2.19), have to be connected to R_{in} at the specific voltage break points, as calculated in equation (2.17). To achieve this, we use another voltage divider:

$$R_{Nn} = R_n \left| \frac{V_{\text{F}} - V_{\text{ref}}}{X_{n-1} - V_{\text{F}}} \right| \text{for } n \geq 2. \tag{2.20}$$

To implement this algorithm, a Python script was written, which is included in the electronic attachment. The LTSpice simulation is shown in figure 2.17. It processes the output of the simulated crossfade input circuit from the previous section.

2.3.5 Irwin linearization scheme

As was discussed in section 2.2.3, SSI2164 provides exponential control over the attenuation of its gain cells:

$$\text{G} = 10^{-V/0.67} \tag{2.21}$$

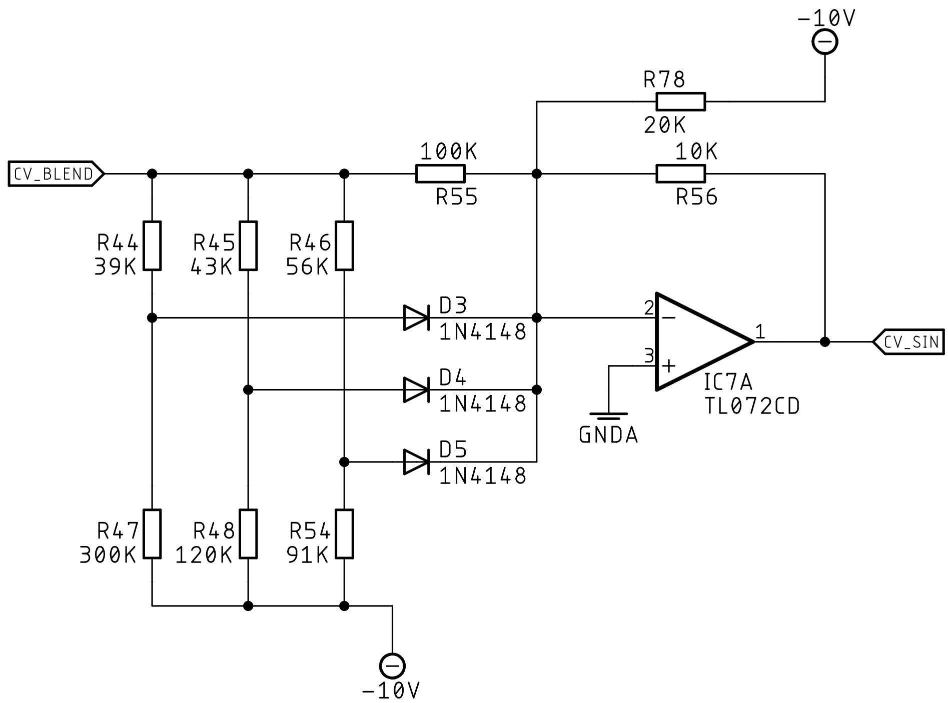

Fig. 2.16: Diode waveshaper

While this behavior is desired in many applications, Eurorack modular synthesizer often operates with linear CVs. In addition, the voltage range of those CVs commonly exceeds the control range of SSI2164. In our case, the *MIX* input expects $-5\,\mathrm{V}$ to $5\,\mathrm{V}$, where $-5\,\mathrm{V}$ is full attenuation and $5\,\mathrm{V}$ is unity gain. To address this, yet another stage of waveshaping based on the Irwin linearization scheme has been adopted from [12] and [18], and is depicted in figure 2.18.

As the name suggests, the Irwin linearization scheme provides a means of linearizing the control response of the SSI2164 gain cells. It does so by incorporating another SSI2164 gain cell into the feedback loop of the op-amp. This amplifier continuously adjusts the VCA, thus generating negative feedback proportionate to the applied voltage on the inputs. By connecting the circuit output to the control port of a normally configured VCA, the exponential control response is exactly corrected, yielding gain control directly proportional to the control voltage. [12]

Even though the amplifier is recommended to be chosen for low offset and low input current to fully utilize the wide dynamic range of SSI2164, a standard TL072H suffices for adequate performance. In this circuit, the output of TL072H is a logarithmic function of the input:

$$V_{\text{out}} = -0.67 \log\left(\frac{-V_{\text{in}}\,R_{21}}{V_{\text{ref}}\,R_{20}}\right), \tag{2.22}$$

where V_{in} is the CV shaped by the diode circuit as discussed in section 2.3.4, and V_{ref} is the negative reference voltage of $-5\,\mathrm{V}$. V_{out} drives the control pin of the

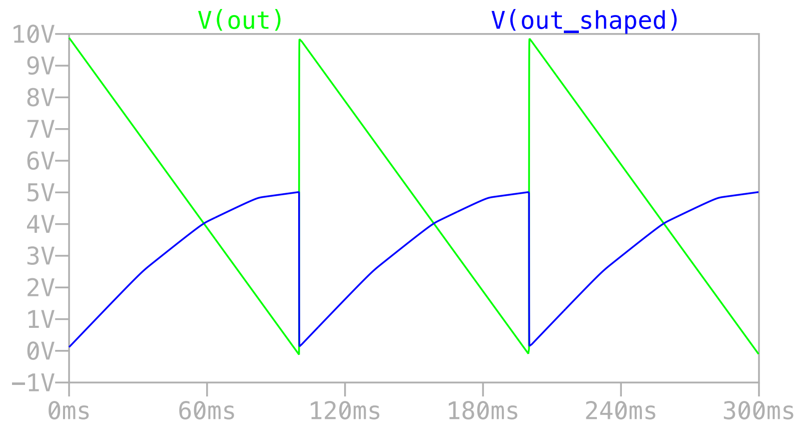

Fig. 2.17: LTSpice simulation of the diode waveshaper

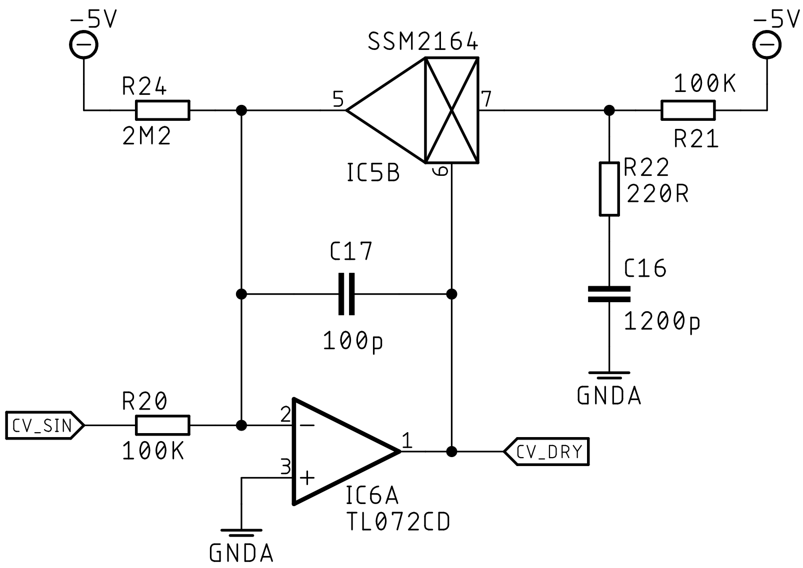

Fig. 2.18: Irwin linearization scheme

gain cell processing the audio signal. Substituting the expression for V_{out} for V in equation (2.21) yields:

$$\text{G} = \frac{V_{\text{in}}\, R_{21}}{V_{\text{ref}}\, R_{20}}, \tag{2.23}$$

which is the linear response we wanted. If $R_{20} = R_{21}$, the expression reduces to

$$\text{G} = \frac{V_{\text{in}}}{V_{\text{ref}}}. \tag{2.24}$$

To achieve thermal and electrical parameter matching, the two gain cells used reside within the same component for each of the signal paths. [12]

The LTSpice simulation is shown in figure 2.19. It processes the output of the simulated crossfade input circuit from the previous section.

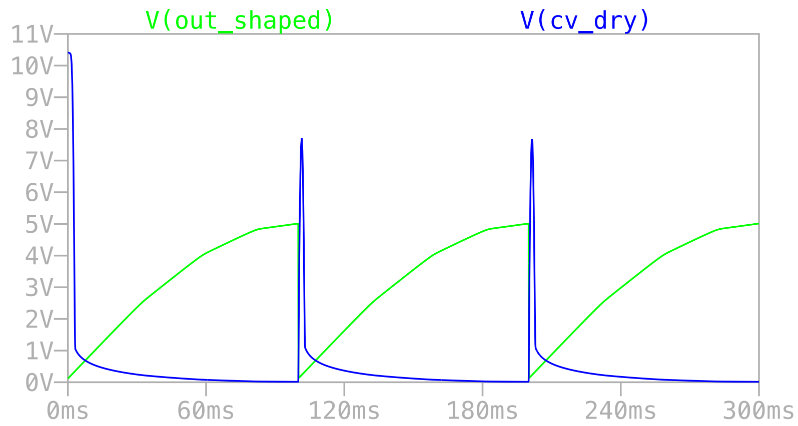

Fig. 2.19: LTSpice simulation of the Irwin linearization scheme

2.3.6 DSP circuit

The datasheet for the FV-1 describes a typical application of the IC with the recommended component values [8]. Figure 2.20 shows the adaptation of this application for the proposed Eurorack module.

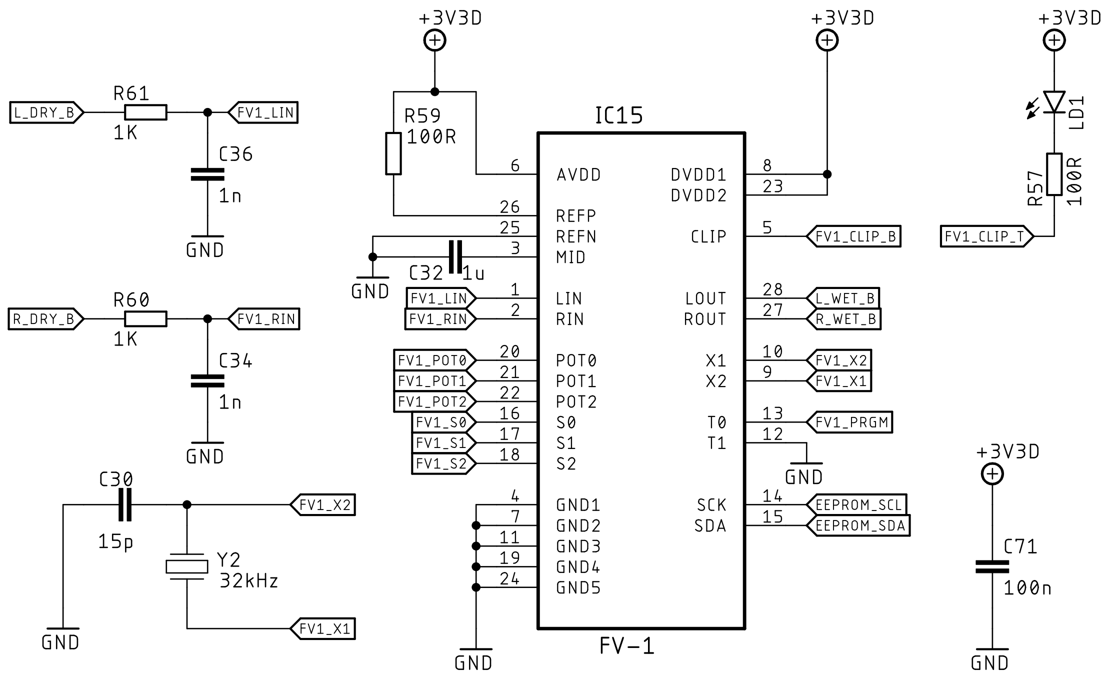

Fig. 2.20: FV-1 application circuit

The FV-1 requires a +3.3 V power, which it receives from the Raspberry Pi Pico.

Audio signals should be brought to FV-1 via coupling capacitors, since the IC does internal biasing of the inputs. These capacitors along with the required gain staging are discussed in section 2.3.1. The datasheet advises to route the input signals through 1 kΩ resistors, coupled with 1 nF NP0 (COG) ceramic capacitors, grounded as closely as possible to the input pins. This should ensure the suppression of any high-frequency noise present in the input signals, and ensure a low impedance at high frequencies.

The clip LED will illuminate for an estimated duration of 30 mS when the internal ADC or DAC reaches a full-scale level by a few tenths of a dB.

All the supply and reference voltage pins should also be bypassed with grounded ceramic capacitors as close to the respective pins as possible.

The standard 32.768 kHz watch crystal oscillator restricts FV-1 frequency response to about 15 kHz. It is recommended to include a 15 pF capacitor between X2 pin and the ground. [8]

Program selection and potentiometer inputs are interfaced with the Raspberry Pi Pico, as will be discussed in section 2.3.7.

2.3.7 MCU circuit

This section describes the schematic design for the Raspberry Pi Pico and the peripheral devices connected to it. These include the user interface elements, such as the display and rotary encoder, but also the circuits that allow it to interface with the FV-1, like the EEPROM and PWM low-pass filters.

To allow safely powering Pico from both the regulator and USB connector, the regulator output is fed into VSYS pin via the FET transistor. The gate of the FET is controlled by VBUS pin, and will disconnect the secondary source when VBUS is present. The P-FET should be chosen to have low on resistance. [9]

Main board

Pico is powered by the +5 V regulator , as will be discussed in section 2.3.9. Internally, it uses a

Display

The display module is a $0,96$" Serial OLED with the resolution of 128×64. It uses a popular SSD1306 single-chip CMOS OLED driver, which has a built-in contrast control, display RAM and oscillator, allowing to reduce the number of external components. [21]

Rotary encoder

Bourns PEC11R-4220K-S0024 is a 2 channel, 24 dent, 24 pulses per revolution (PPR) rotary encoder with a push-button. It's powered by +5 V and requires pull-up resistors on all of its pins. A typical application of the encoder with the

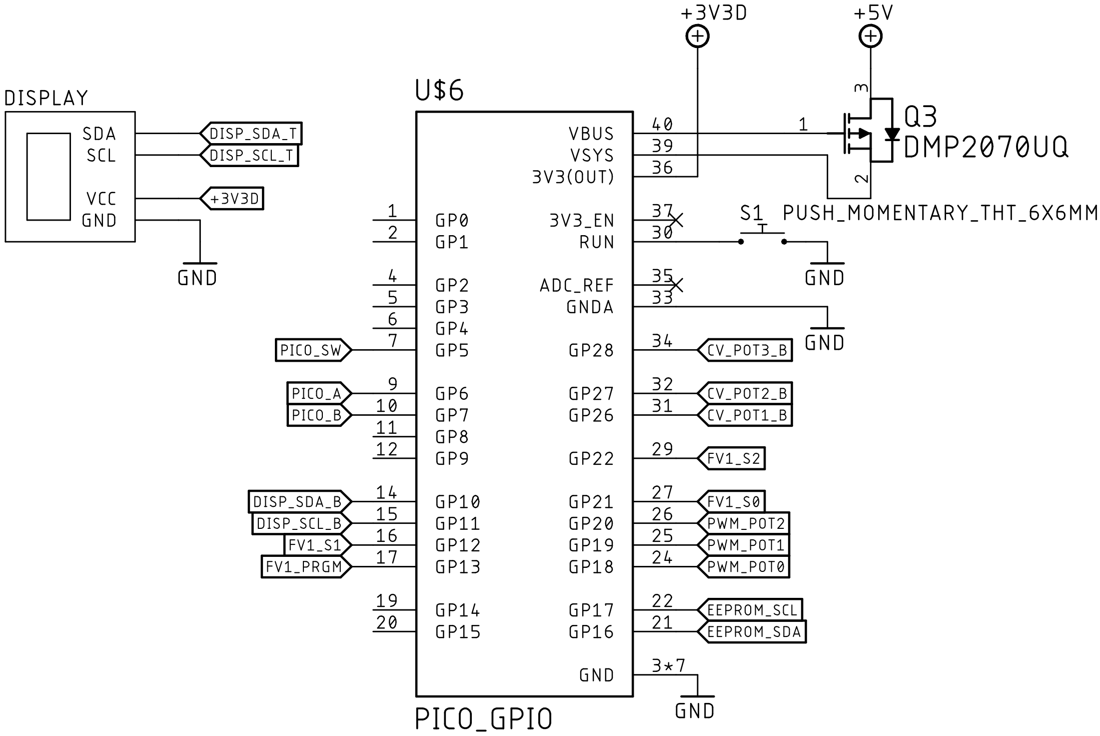

Fig. 2.21: Raspberry Pi Pico application circuit

recommended component values is provided in the datasheet [22] and is shown in figure 2.22.

EEPROM

The EEPROM model was chosen based on the FV-1 datasheet [8]. The Microchip Technology Inc. 24LC64 is a 64Kb Serial EEPROM. It is organized as a single block of 8K x 8-bit memory with a 2-wire serial interface. [20] It's connected to both the Pico and the FV-1 to allow for dynamic programming of the effects IC.

PWM DAC circuit

To allow for more flexibility in the design, rather than connecting the control inputs of the FV-1 directly to the potentiometers, they are connected to the digital pins of the MCU. Even though the RP2040 microcontroller lacks a Digital-to-Analog Converter (DAC), it has 8 independent PWM slices, where each slice can control two PWM outputs (A and B). The two outputs from a single slice share a common clock divider and a counter, but have independent control inputs, which allows setting different duty cycles for each output. [19] It is possible to use these PWM slices to create analog output by combining them with a low-pass filter. [23]

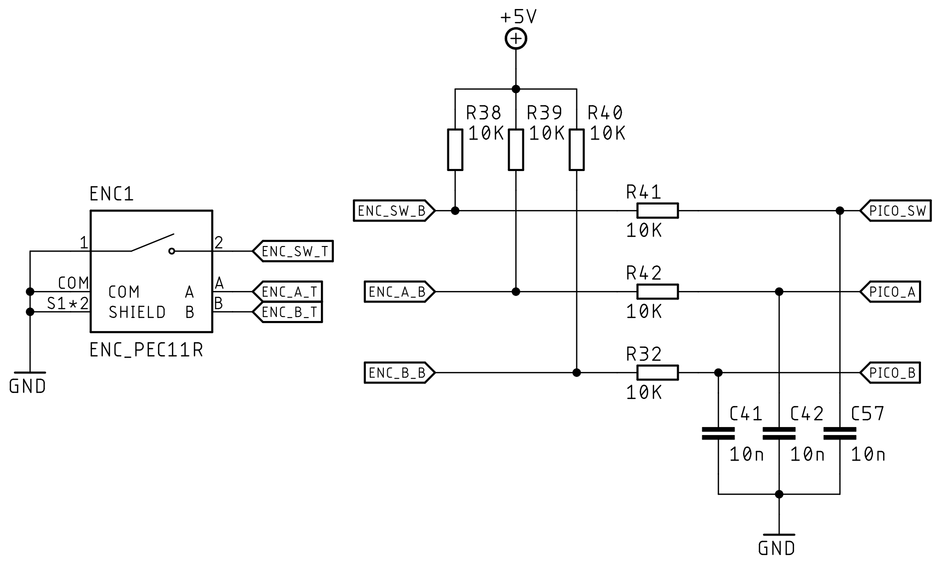

Fig. 2.22: Encoder application circuit

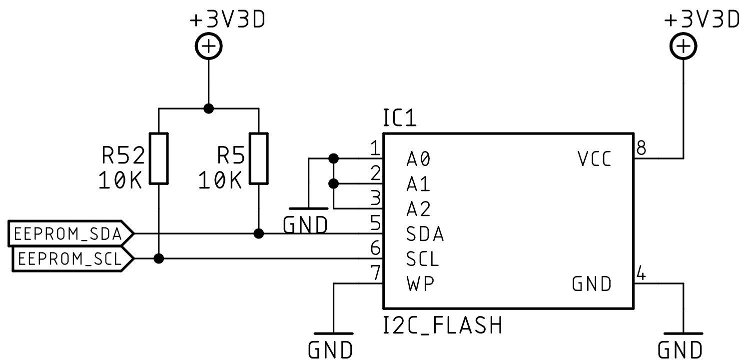

Fig. 2.23: EEPROM connection

Even though a second-order filter is generally recommended to suppress ripple-voltages while preserving fast onset times, it introduces additional complexity and cost. As discussed in section 2.2.1, the FV-1 features built-in hysteresis for each of its potentiometer inputs, which makes fluctuations of the CV more permissible. Therefore, a simple RC-filter has been used, as shown in figure 2.24.

To minimize the ripple voltage, the bandwidth of the analog signal has been chosen two orders of magnitude lower than the PWM frequency $f_{\mathrm{PWM}} = 100\,\mathrm{kHz}$. For a simple RC-filter, a *time constant* is given by

$$\tau = RC = \frac{1}{2\pi f_{\mathrm{c}}}, \tag{2.25}$$

where f_{c} is a *cut-off frequency* of the filter. If the capacitor value is $C = 100\,\mathrm{nF}$, the resistor value should be

$$R = \frac{1}{2\pi f_{\mathrm{c}} C} = \frac{1}{2\pi \cdot 100\,\mathrm{kHz} \cdot 100\,\mathrm{nF}} = 1591.55\,\Omega. \tag{2.26}$$

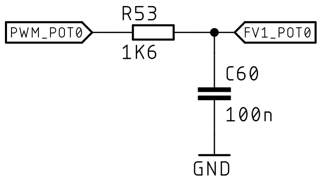

Fig. 2.24: PWM DAC

The actual value was chosen as the closest E24 series value of 1600 Ω.

2.3.8 Audio outputs

The output circuit brings together the outputs of circuits described in sections 2.3.1, 2.3.5 and 2.3.6. The design of each audio signal path is essentially identical to the input, which was discussed in section 2.3.1, with the values of input and feedback resistors swapped. Once again, only the left channel is described, as the right one is identical. These jack sockets correspond to the *L OUT* and *R OUT* outputs on the panel.

Shown in figure 2.25, the circuit works as a two-into-one-mixer, where two VCA outputs are summed together into a single op-amp. [12] Resistor pairs R_8 and R_{29}, and R_{62} and R_{29} ensure that the signal is brought back from internal $3\,\mathrm{V_{pp}}$ to the standard Eurorack signal level of $10\,\mathrm{V_{pp}}$.

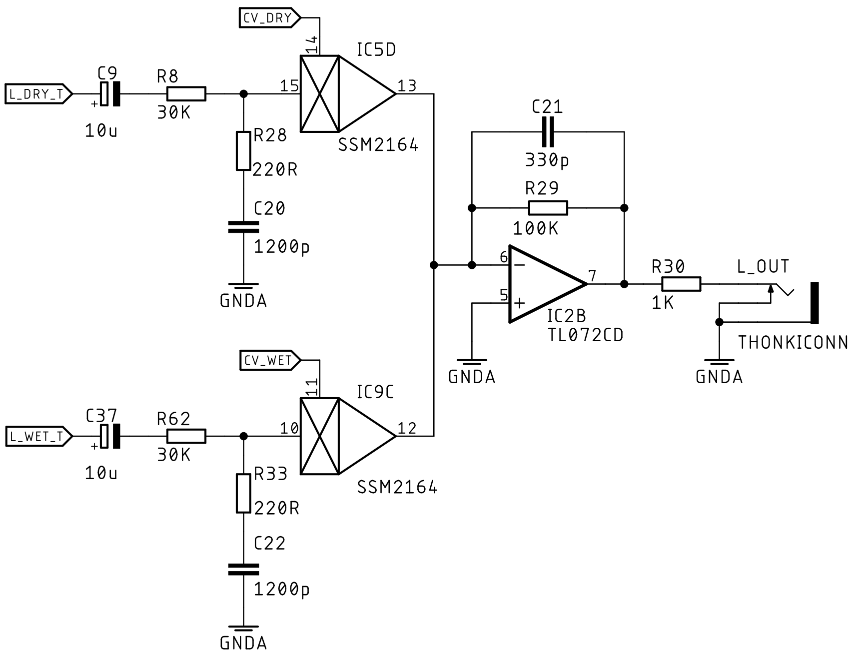

Fig. 2.25: Left output circuit

The output resistor $R_{30} = 1\,\mathrm{k}\Omega$ ensures, that the output impedance of the module conforms with the Eurorack standards, as discussed in section 1.2.2.

The circuit was simulated in LTSpice with $3\,\mathrm{V_{pp}}$ $1\,\mathrm{kHz}$ sine and cosine signals, which corresponds to a maximum signal level one may expect from the FV-1 output (per table 2.1). The result of the simulation is shown in figures 2.26 and 2.27. First, we test the output for a crossfader at on one of its extremes. As expected, only one of the input signals is brought to the Eurorack level, and the other one is attenuated. When the crossfader is in the middle, both sine and cosine are equally loud, and so the output signal cancels out.

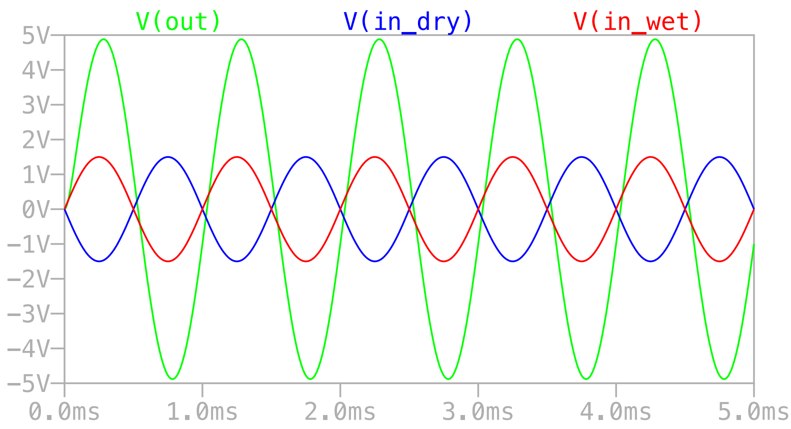

Fig. 2.26: LTSpice simulation of the output, crossfader in the extreme position

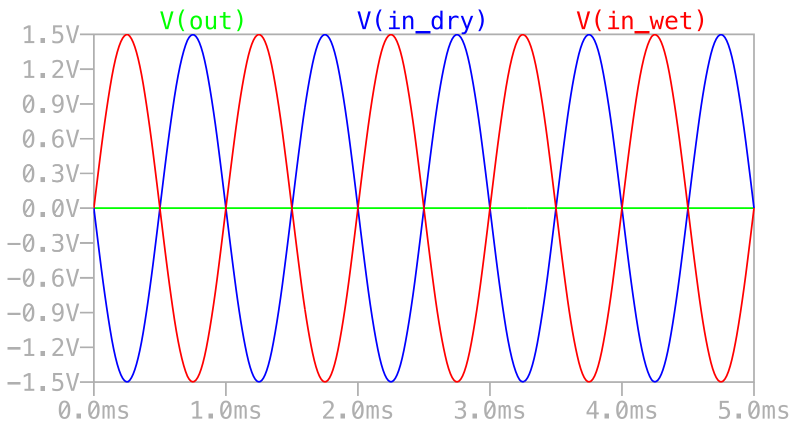

Fig. 2.27: LTSpice simulation of the output, crossfader in the middle position

2.3.9 Power supply and reference volatges

The module is powered by the Eurorack synthesizer power supply through a 2×5 pin header power connector, which usually delivers $\pm 12\,\mathrm{V}$ and common ground GND, as was discussed in section 1.2.2. The power connector circuit is shown in Figure 2.28. Each voltage branch features PPTC and rectifier diodes to provide current and polarity reversal protection. To protect against power supply voltage spikes, bypass capacitors are used.

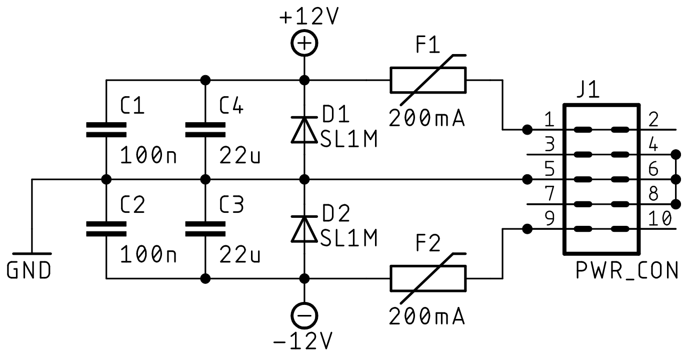

Fig. 2.28: Eurorack power connector

±12 V is used to power the TL072H op-amps and SSI2164 VCAs. To circumvent possible current spikes, 100 nF coupling capacitors were used for every power input in the circuit. An example of the typical power connection from the schematic is shown in figure 2.29.

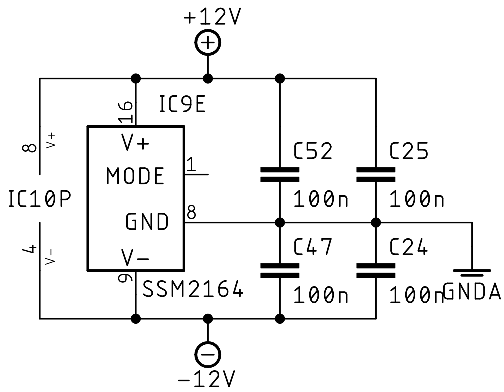

Fig. 2.29: Typical power connection of the TL072H and SSI2164

Figure 2.30 shows the power regulators used for the rest of the circuit. For powering the single-supply MCP6002 op-amps, a voltage of +3.3V is provided by the Texas Instruments 800 mA 15 V linear voltage regulator LM1117IDTX-3.3. As per its datasheet, a pair of bypass capacitors is present on both the input and the output to protect it against voltage fluctuations. [24]

The Texas Instruments 800 mA 15 V linear voltage regulator LM1117IDTX-5.0 supplies +5 V power to the Raspberry Pi Pico and the rotary encoder. To reduce the risk of noise and interference between analog and digital circuitry, separate power supplies and ground planes were used for the analog and digital circuits.

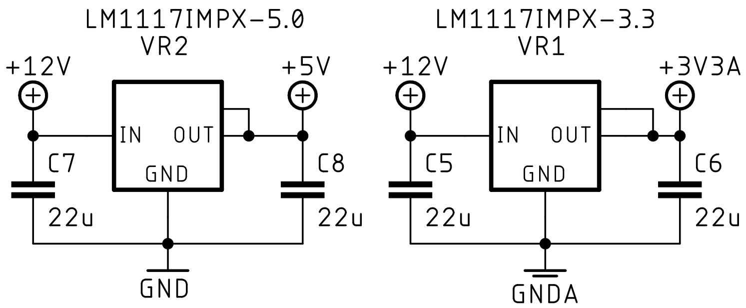

Fig. 2.30: Voltage regulators

The proposed circuit requires two reference voltages. The −5 V reference voltage is required for the Irwin linearization circuit from section 2.3.5, and the −10 V reference voltage is used for the voltage offsets (sections 2.3.2, 2.3.3 and 2.3.4) and in the diode wave shaper to define the required break points (section 2.3.4).

The LM4040-N series of shunt reference voltages offers low dynamic impedance, low noise, and low temperature coefficient to ensure a stable output voltage over a wide range of operating currents and temperatures.

A conventional shunt reference application is shown in figure 2.31, where the series resistor R_S connects the supply voltage V_S and the LM4040-N. R_S determines the current I_L that flows through the load and the current I_Q that flows through the LM4040-N:

$$R_\mathrm{S} = \frac{V_\mathrm{S} - V_\mathrm{R}}{I_\mathrm{L} + I_\mathrm{Q}}, \tag{2.27}$$

where V_R is the reverse breakdown voltage that will serve as the reference voltage.

I_L and V_S may vary, so R_S must be small enough to supply LM4040-N with at least the minimum acceptable $I_{\mathrm{Q,\ min}}$, even when V_S is at its minimum and I_L is at its maximum:

$$R_{\mathrm{S,\ max}} = \frac{V_{\mathrm{S,\ min}} - V_\mathrm{R}}{I_{\mathrm{L,\ max}} + I_{\mathrm{Q,\ min}}}. \tag{2.28}$$

When V_S is at its maximum and I_L is at its minimum, R_S should be large enough so that the maximum acceptable $I_{\mathrm{Q,\ max}}$ is less than 15 mA:

$$R_{\mathrm{S,\ min}} = \frac{V_{\mathrm{S,\ max}} - V_\mathrm{R}}{I_{\mathrm{L,\ min}} + I_{\mathrm{Q,\ max}}}. \tag{2.29}$$

To simplify calculations, we'll assume that the load current can drop to zero without affecting the functionality of the system. This way, $I_{\mathrm{L,\ min}}$ would always be 0 µA. Potential fluctuations of the supply voltage are similarly not accounted for, therefore $V_{\mathrm{S,\ min}} = V_{\mathrm{S,\ max}} = V_\mathrm{S} = -12\,\mathrm{V}$. [25]

For the −5 V reference, the maximum load current $I_{\mathrm{L,\ max}}$ is determined by R_{21} and R_{R24} from the Dry CV signal path (figure 2.18), and the identical pair of values

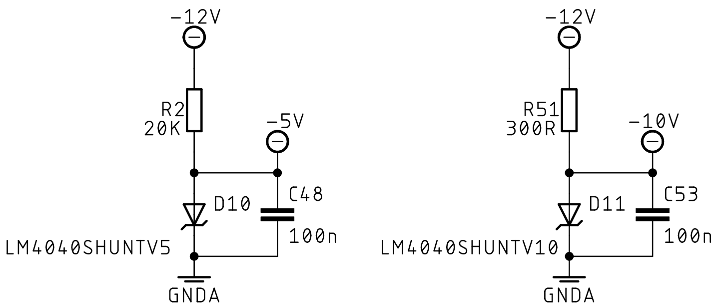

Fig. 2.31: Shunt reference voltages

from the Wet CV signal path. We can then simply use the Ohms' law to determine the maximum load current

$$I_{\mathrm{L,\,max}} = \left(\frac{V_\mathrm{R}}{R_{21}} + \frac{V_\mathrm{R}}{R_{24}}\right) \cdot 2 = \left(\frac{-5\,\mathrm{V}}{100\,\mathrm{k\Omega}} + \frac{-5\,\mathrm{V}}{2.2\,\mathrm{M\Omega}}\right) \cdot 2 = -104.55\,\mathrm{\mu A}. \tag{2.30}$$

R_S should be in the range from

$$R_{\mathrm{S,\,min}} = \frac{V_{\mathrm{S,\,max}} - V_\mathrm{R}}{I_{\mathrm{L,\,min}} + I_{\mathrm{Q,\,max}}} = \frac{-12\,\mathrm{V} + 5\,\mathrm{V}}{0\,\mathrm{\mu A} - 15\,\mathrm{mA}} = 466.67\,\Omega \tag{2.31}$$

to

$$R_{\mathrm{S,\,max}} = \frac{V_{\mathrm{S,\,min}} - V_\mathrm{R}}{I_{\mathrm{L,\,max}} + I_{\mathrm{Q,\,min}}} = \frac{-12\,\mathrm{V} + 5\,\mathrm{V}}{-104.55\,\mathrm{\mu A} - 80\,\mathrm{\mu A}} = 37930.1\,\mathrm{k\Omega}, \tag{2.32}$$

and was set to $20\,\mathrm{k\Omega}$.

For the $-10\,\mathrm{V}$ reference, the maximum load current $I_{\mathrm{L,\,max}}$ is determined by the potentiometers of the CV inputs (figure 2.8), the potentiometer and the offset resistor R_{77} of the crossfader input (figures 2.10 and 2.12), as well as the offset (R_{78}) and voltage divider resistors of the diode wave shapers (figure 2.16). All mentioned resistances are connected between $-10\,\mathrm{V}$ and $0\,\mathrm{V}$, so the total conductance is

$$\begin{aligned} G &= \frac{4}{R_{\mathrm{P1}}} + \frac{1}{R_{77}} + \frac{2}{R_{78}} + \frac{2}{R_{44} + R_{47}} + \frac{2}{R_{45} + R_{48}} + \frac{2}{R_{46} + R_{54}} \\ &= \frac{4}{10\,\mathrm{k\Omega}} + \frac{1}{100\,\mathrm{k\Omega}} + \frac{2}{20\,\mathrm{k\Omega}} + \frac{2}{(39+300)\,\mathrm{k\Omega}} + \frac{2}{(43+120)\,\mathrm{k\Omega}} + \frac{2}{(56+91)\,\mathrm{k\Omega}} \\ &= 541.78\,\mathrm{\mu S}. \end{aligned} \tag{2.33}$$

The maximum load current is then simply

$$I_{\mathrm{L,\,max}} = G\,V_\mathrm{R} = 541.78\,\mathrm{\mu S} \cdot (-10\,\mathrm{V}) = -5.42\,\mathrm{mA}. \tag{2.34}$$

R_S should be in the range from

$$R_{\mathrm{S,\,min}} = \frac{V_{\mathrm{S,\,max}} - V_\mathrm{R}}{I_{\mathrm{L,\,min}} + I_{\mathrm{Q,\,max}}} = \frac{-12\,\mathrm{V} + 10\,\mathrm{V}}{0\,\mathrm{\mu A} - 15\,\mathrm{mA}} = 133.33\,\Omega \tag{2.35}$$

to

$$R_{\mathrm{S,\ max}} = \frac{V_{\mathrm{S,\ min}} - V_{\mathrm{R}}}{I_{\mathrm{L,\ max}} + I_{\mathrm{Q,\ min}}} = \frac{-12\,\mathrm{V} + 10\,\mathrm{V}}{-5.42\,\mathrm{mA} - 105\,\mathrm{\mu A}} = 361.99\,\Omega, \tag{2.36}$$

and was set to $300\,\Omega$.

2.4 PCB design

The PCB design was created using the PCB design and schematic software Autodesk EAGLE 9.6.2.

The schematic was divided into two boards. The top board contains all the user-facing components, like jacks and sliders, the display and the rotary encoder, but also all the analog circuitry like the input and output VCAs and op-amps. The bottom board contains the power connector and digital components like the Raspberry Pi Pico and the FV-1.

The proposed design uses both through-hole ans surface-mount technologies. All the user-facing components are realized as through-hole devices, while most of the integrated electronics are surface-mount. The Raspberry Pi Pico is connected to the bottom board using through-hole pins. The display is connected to the top board using through-hole pins as well. For both boards, the surface mount devices are placed on a single side of the PCB, while through-hole components are placed on the opposite side.

While designing the PCB, care was taken to separate analog, digital, and power sections of the circuit. Individual power lanes are routed using wider traces to minimize voltage drops and maximize heat dissipation. Grounding is implemented through a ground plane that fills the entire surface of each board. The ground planes of the analog and digital circuits are separated, per the discussion in section 2.3.9, and are connected via a single solder jumper on the bottom board.

The entire PCB design can be found in the appendix. The PCB layout of the boards is shown in figures B.1 and B.2. An assembly view of the boards is shown in figures B.3 and B.4.

2.5 Panel design

The initial panel design, as presented in figure 2.1, was created using Inkscape 1.2.2. Panel dimensions are in accordance with the mechanical specifications of the Eurorack modular synthesizer, which were discussed in section 1.2.2.

2.6 Programming

The 2-wire Serial Wire Debug (SWD) port of the Raspberry Pi Pico was used to get access to hardware and software debug features, such as automatically reloading the board and flashing new firmware into memory. The SWD bus is exposed on two dedicated pins – SWCLK and SWDIO. SWCLK carries a clock signal from the debugger, while SWDIO is used for bidirectional transfer of serial data. For debugging and programming the Pico, another Raspberry Pi Pico with *picoprobe* firmware was used. The software was developed in Microsoft Visual Studio Code using C++.

2.6.1 Main program structure

The program starts execution in the `main()` function, where the initialization function is called. It sets up all the hardware of the module, like the display, encoder, serial buses, pins and PWM.

Then programs from the included ROM file are loaded into the EEPROM memory using the I2C interface.

The program then enters an infinite loop, where it continuously performs a set of tasks:

- If the rotary encoder is pressed, the program bank is toggled between the internal ROM and the external EEPROM
- If the rotary encoder is rotated, a new FV-1 program is set by the program pins
- Potentiometer values connected to the ADC are continuously read and transformed into the PWM output
- The display is refreshed at a certain rate or whenever necessary

The current program name and parameters are displayed using the display function.

Conclusion

The aim of this work was to study Digital Signal Processing and its application in the embedded context of modular synthesis using the programmable effect chip Spin Semiconductor FV-1. The implementation part of this thesis was first devoted to studying properties and parameters of the IC. The unique instruction set along with the parallel nature of the FV-1 operations makes it uniquely qualified in the realm of affordable digital audio processors. While the chip offers many unique capabilities, such as native support for logarithm and exponent operations, or two-instruction filter designs, it is limited in several key aspects. For one, it allows for only three parameters to be controlled. Furthermore, it supports only 8 user programs. Additionally, there is no preset memory or mixing control, which means that at least one of the control parameters would have to be sacrificed to solve such tasks digitally. Some of these problems can be solved by the introduction of microcontroller unit. Therefore, a Raspberry Pi Pico was employed. This addition allowed to also include a display for better communication of effect names and parameters. The microcontroller unit is also used to serially write new programs to the EEPROM FV-1 is connected to, thus realizing the programmable aspect of this effect processor. The FV-1 and Pico are additionally interfaced in other key ways. The program selection pins of the FV-1 are directly connected to Pico, allowing the latter to determine which effect is currently loaded in FV-1 memory. The DSP parameters of the FV-1 are similarly controlled by the Pico. To achieve this, the control voltages are first read by the ADC of Pico, and then PWM along with the passive low-pass filter are used.

To solve the problem with signal mixing, a fully analog signal path has been designed. While a simple linear crossfader is easily achievable, the peculiarities of human hearing and the linear nature of Eurorack control voltages required a more nuanced approach. Firstly, a problem of non-coherent signal mixing had to be solved. When two such signals are crossfaded, a noticeable decrease in loudness occurs in the middle position of the fader. The chosen solution was to employ a constant power mixing law, where the volume CVs are shaped in a way, where their sum always results in equal perceived loudness. To achieve this, a diode waveshaper has been designed. The next challenge lied in the particular control characteristics of the employed VCA. While modular signals are generally linear, SSI2164 provides exponential control over its attenuation. Therefore, an Irwin linearization scheme has been constructed. This circuit allows using that same VCA in the feedback path of the op-amp to take the logarithm of the incoming signal. This way, when exponential input of the VCA processes such signal, and the components are chosen appropriately, the control characteristic essentially becomes linear with regard to the input signal.

There are numerous avenues which may be explored further. Firstly, while the diode waveshaper works well enough for two signals of the same volume, it is not always guaranteed that that would be the case. For example, some effect algorithms may produce lower voltages based on the currently selected settings. In such cases, the constant power mixing law would no longer hold true. Additionally, if the input signals were actually coherent, $-3\,\mathrm{dB}$ law would start amplifying such signals in the center position of the slider. Thus, a much better solution would be to tackle this problem digitally. By employing a DAC, the microprocessor would be able to control the attenuation curve of the VCA dynamically, which would allow solving the mixing problem on a case-by-case basis. It would also greatly simplify the circuit design, as there would be no need for complicated analog waveshaping schemes.

While the use of the ready-made microcontroller board greatly simplified the prototyping process, it proved to be challenging to incorporate such a board into the relatively constrained footprint of the Eurorack module. Furthermore, it made it much more difficult to properly divide analog and digital signal paths. Thus, a completely integrated approach seems much more desirable.

Even though the provided code is sufficient for simple program switching, it can potentially greatly expand the capabilities of FV-1. For example, additional digital modulators can be introduced, or a preset system may be added.

Bibliography

[1] LOY, Gareth. *Musimathics: the Mathematical Foundations of Music*. Vol. 1. Cambridge, MA: MIT Press, 2006. ISBN 978-0-262-12282-5.

[2] BJØRN, Kim and MEYER, Chris. *PATCH & TWEAK: Exploring Modular Synthesis*. Denmark: Bjooks, 2018. ISBN 978-87-999995-1-4.

[3] Doepfer Musikelektronik GmbH. [online manual]. *SYSTEM A-100 Owner's Manual*. 2003. [Accessed 20.05.2023]. Available from: `https://doepfer.de/a100_man/A100_Manual_complete.pdf`

[4] Doepfer Musikelektronik GmbH. [online]. *A-100 Standard Systems*. [Accessed 20.05.2023]. Available from: `https://doepfer.de/a100s_e.htm`

[5] Doepfer Musikelektronik GmbH. [online manual]. *A-100 Construction Details*. [Accessed 20.05.2023]. Available from: `https://doepfer.de/a100_man/a100m_e.htm`

[6] ZÖLZER, Udo, ed. *DAFX: Digital Audio Effects*. 2nd ed. Chichester: Wiley. 2011. ISBN 978-0-470-66599-2.

[7] Spin Semiconductor. [online knowledge base]. *Informal Notes on DSP using the FV-1 Signal Processor*. 2018. [Accessed 05.05.2023]. Available from: `http://www.spinsemi.com/knowledge_base.html`

[8] Spin Semiconductor. [online datasheet]. *Data sheet for the FV-1 (SPN1001)*. 2017. [Accessed 05.05.2023]. Available from: `http://www.spinsemi.com/Products/datasheets/spn1001/FV-1.pdf`

[9] Raspberry Pi Ltd. [online datasheet]. *Raspberry Pi Pico Datasheet: An RP2040-based microcontroller board*. 2023. [Accessed 10.05.2023]. Available from: `https://datasheets.raspberrypi.com/pico/pico-datasheet.pdf`

[10] Texas Instruments Incorporated. [online datasheet]. *TL07xx Low-Noise FET-Input Operational Amplifiers*. 2023. [Accessed 14.05.2023]. Available from: `https://www.ti.com/lit/ds/symlink/tl071h.pdf`

[11] Microchip Technology Inc. [online datasheet]. *MCP6001/2/4 1 MHz, Low-Power Op Amp*. 2020. [Accessed 14.05.2023]. Available from: `https://ww1.microchip.com/downloads/aemDocuments/documents/MSLD/ProductDocuments/DataSheets/MCP6001-1R-1U-2-4-1-MHz-Low-Power-Op-Amp-DS20001733L.pdf`

[12] Sound Semiconductor Inc. [online datasheet]. *SSI2164 FATKEYS^{TM} QUAD VOLTAGE CONTROLLED AMPLIFIER*. 2023. [Accessed 10.05.2023]. Available from: `https://soundsemiconductor.com/downloads/ssi2164datasheet.pdf`

[13] HOROWITZ, Paul and HILL, Winfield. *The Art of Electronics*. 3rd edition. New York: Cambridge University Press, 2015. ISBN 9780521809269.

[14] Texas Instruments Incorporated. [online application report]. *Amplifier Circuit Collection (rev. D)*. 2019. [Accessed 10.05.2023]. Available from: `https://www.ti.com/lit/pdf/snla140`

[15] SCHIMMEL, Jiří. *Elektroakustika*. Brno: Brno University of Technology. 2016. ISBN 978-80-214-4716-5

[16] VRBA, Kamil and MIŠUREC, Jiří. *Technika analogových obvodů*. Brno: Brno University of Technology. VUTIUM, 2020. ISBN 978-80-214-5901-4.

[17] HANÁK, Pavel and KUBÁNEK, David. *Analogová technika. Laboratorní cvičení*. Brno: Brno University of Technology. 2021.

[18] EDN.com. [online article]. *Op amp linearizes attenuator control response*. 2002. [Accessed 14.05.2023]. Available from: `https://www.edn.com/op-amp-linearizes-attenuator-control-response/`

[19] Raspberry Pi Ltd. [online datasheet]. *RP2040: A microcontroller by Raspberry Pi*. 2023. [Accessed 10.05.2023]. Available from: `https://datasheets.raspberrypi.com/rp2040/rp2040-datasheet.pdf`

[20] Microchip Technology Inc. [online datasheet]. *24AA64/24FC64/24LC64 64-Kbit I^{2}C Serial EEPROM*. 2022. [Accessed 07.05.2023]. Available from: `https://ww1.microchip.com/downloads/aemDocuments/documents/MPD/ProductDocuments/DataSheets/24AA64-24FC64-24LC64-64-Kbit-I2C-Serial-EEPROM-20001189U.pdf`

[21] SOLOMON SYSTECH. [online datasheet]. *SSD1306 128×64 Dot Matrix OLED/PLED Segment/Common Driver with Controller*. 2008. [Accessed 04.05.2023]. `https://cdn-shop.adafruit.com/datasheets/SSD1306.pdf`

[22] Bourns, Inc. [online datasheet]. *PEC11R Series – 12 mm Incremental Encoder*. 2023. [Accessed 01.05.2023]. Available from: `https://www.bourns.com/docs/product-datasheets/pec11r.pdf`

[23] Microchip Technology Inc. [online application note]. *Using PWM to Generate an Analog Output*. 2020. [Accessed 18.05.2023]. Available from: `https://ww1.microchip.com/downloads/en/Appnotes/90003250A.pdf`

[24] Texas Instruments Incorporated. [online datasheet]. *LM1117 800-mA, Low-Dropout Linear Regulator*. 2023. [Accessed 12.05.2023]. Available from: `https://www.ti.com/lit/ds/symlink/lm1117.pdf`

[25] Texas Instruments Incorporated. [online datasheet]. *LM4040-N/-Q1 Precision Micropower Shunt Voltage Reference*. 2016. [Accessed 14.05.2023]. Available from: `https://www.ti.com/lit/ds/symlink/lm4040-n.pdf`

Symbols and abbreviations

DSP Digital Signal Processing

SPL Sound Pressure Level

p root-mean-square value of the sound pressure

CV Control Voltage

LFO Low Frequency Oscillator

VCF Voltage-Controlled Filter

HPF High-Pass Filter

LPF Low-Pass Filter

VCA Voltage-Controlled Amplifier

VCO Voltage-Controlled Oscillator

LPG Low-Pass Gate

U rack unit

HP horizontal pitch units

PCB Printed Circuit Board

ADC Analog-to-Digital Converter

DAC Digital-to-Analog Converter

RAM Random-Access Memory

ROM Read-Only Memory

EEPROM Electrically Erasable Programmable Read-Only Memory

MCU Microcontroller Unit

LED Light Emitting Diode

SWD Serial Wire Debug

$\mathrm{V_{pp}}$ Volt peak-to-peak

List of appendices

A Schematic diagrams

A.1 Power

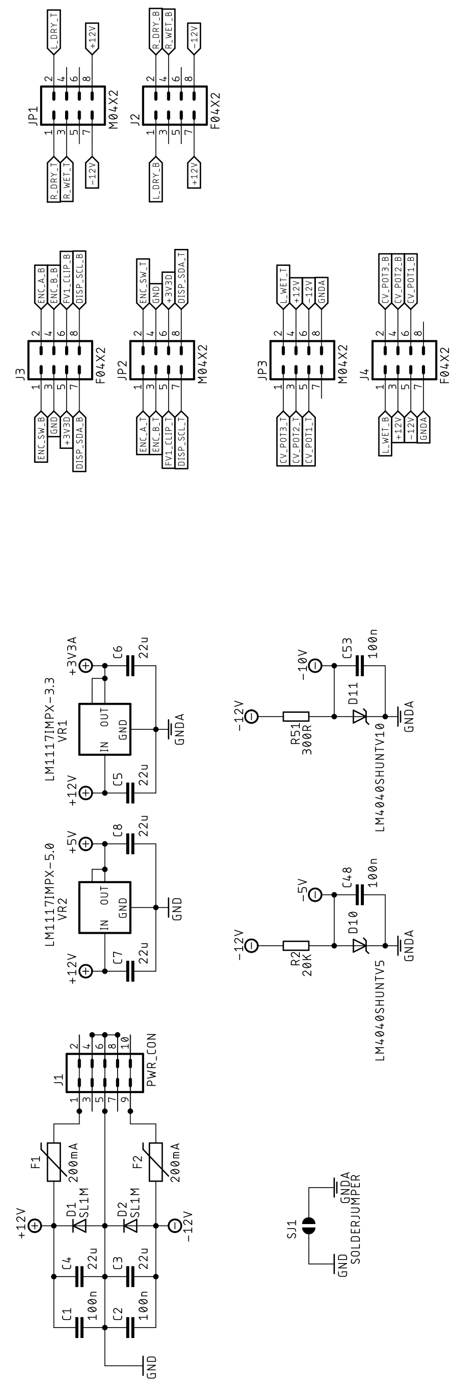

Fig. A.1: Schematic diagram of the power circuit

A.2 Analog circuit

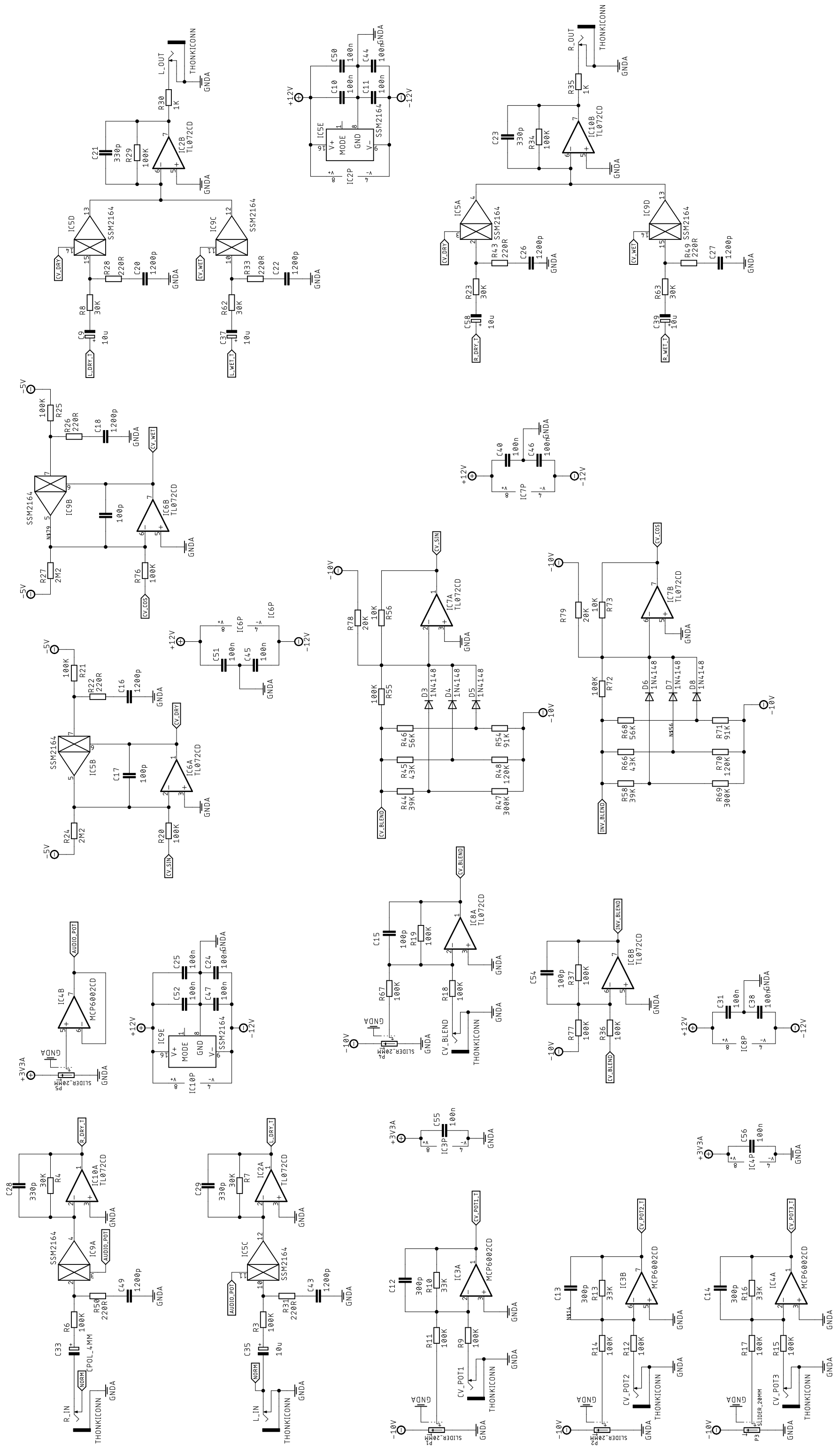

Fig. A.2: Schematic diagram of the analog circuit

A.3 Digital circuit

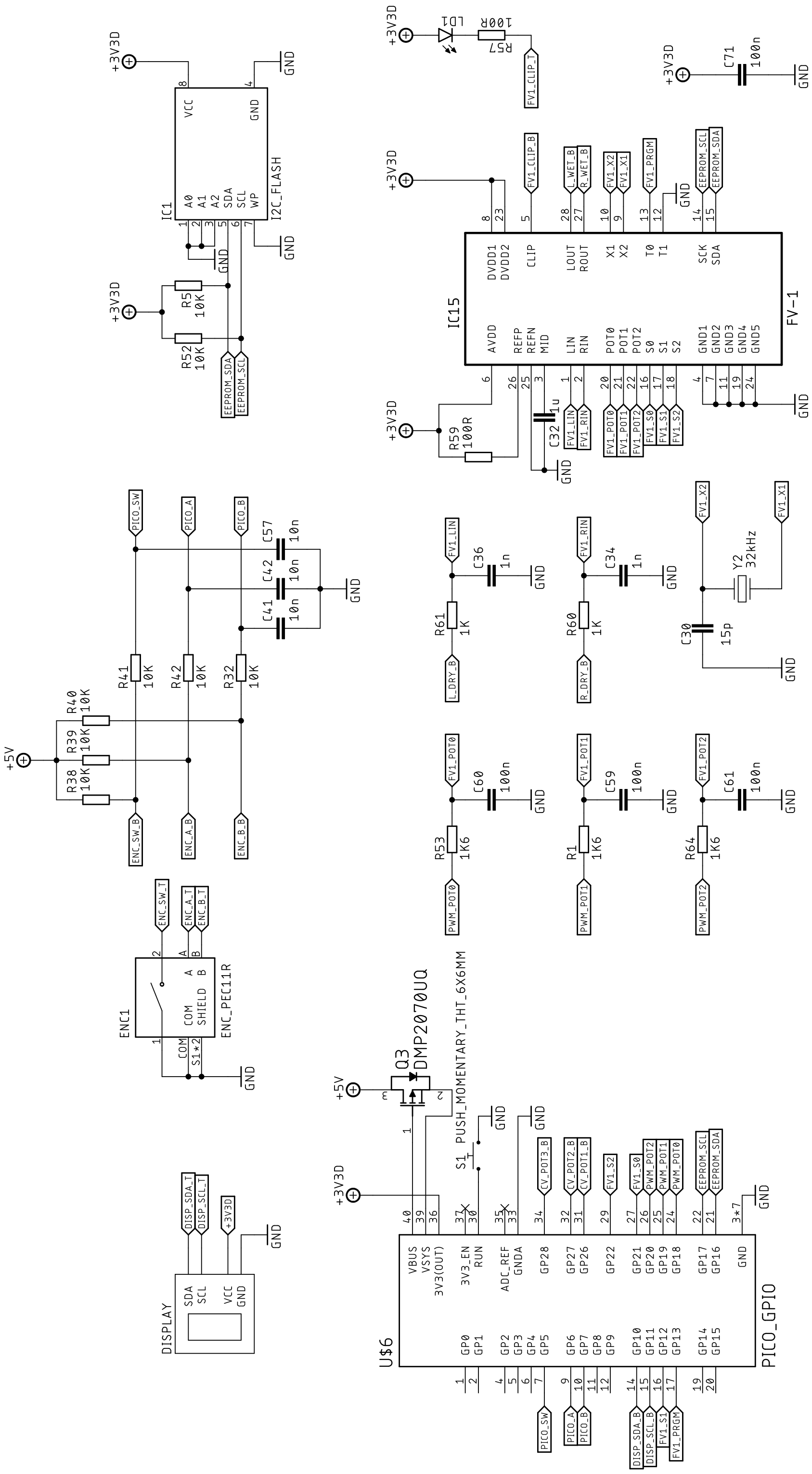

Fig. A.3: Schematic diagram of the digital circuit

B PCB design

B.1 PCB – top

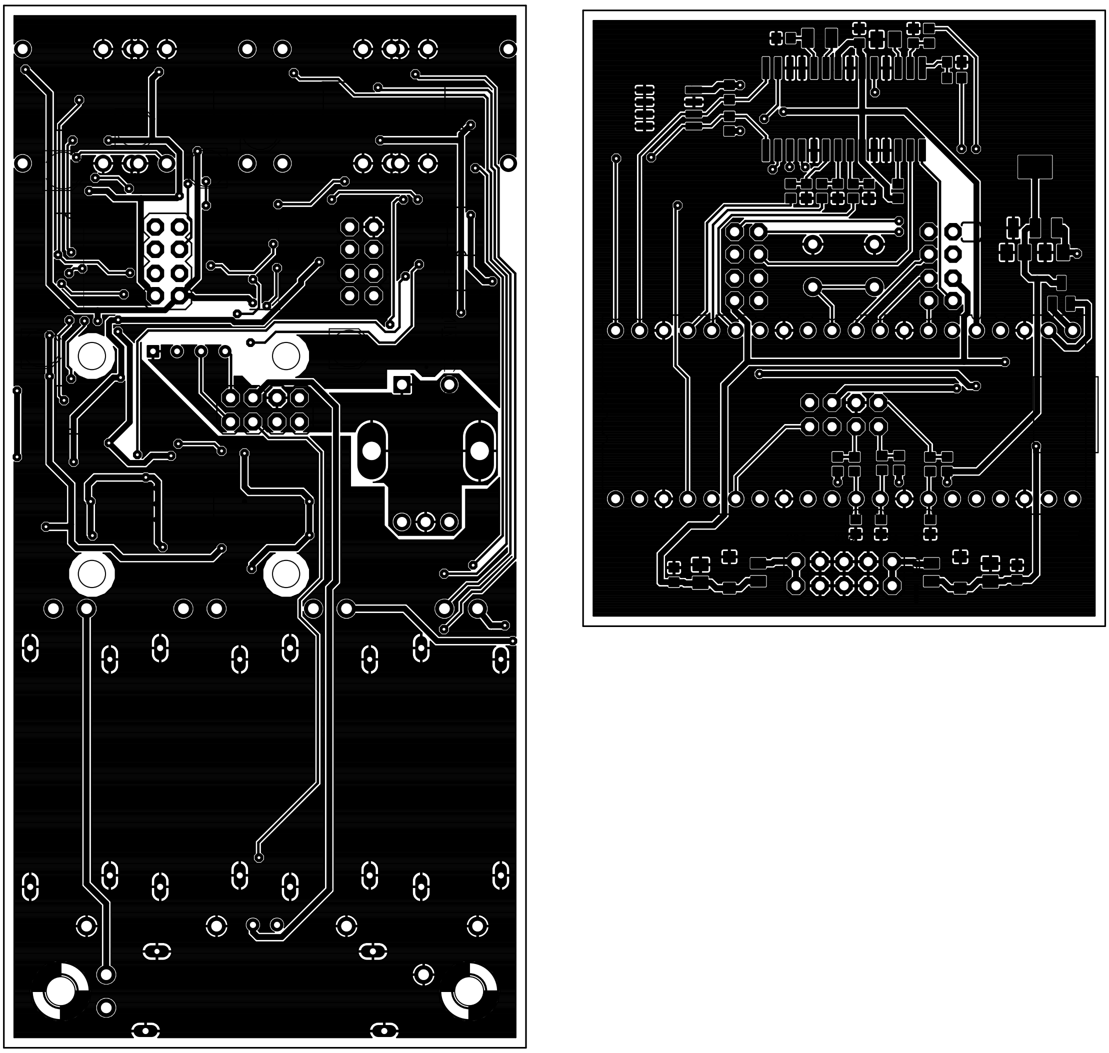

Fig. B.1: Top layer of the PCB

B.2 PCB – bottom

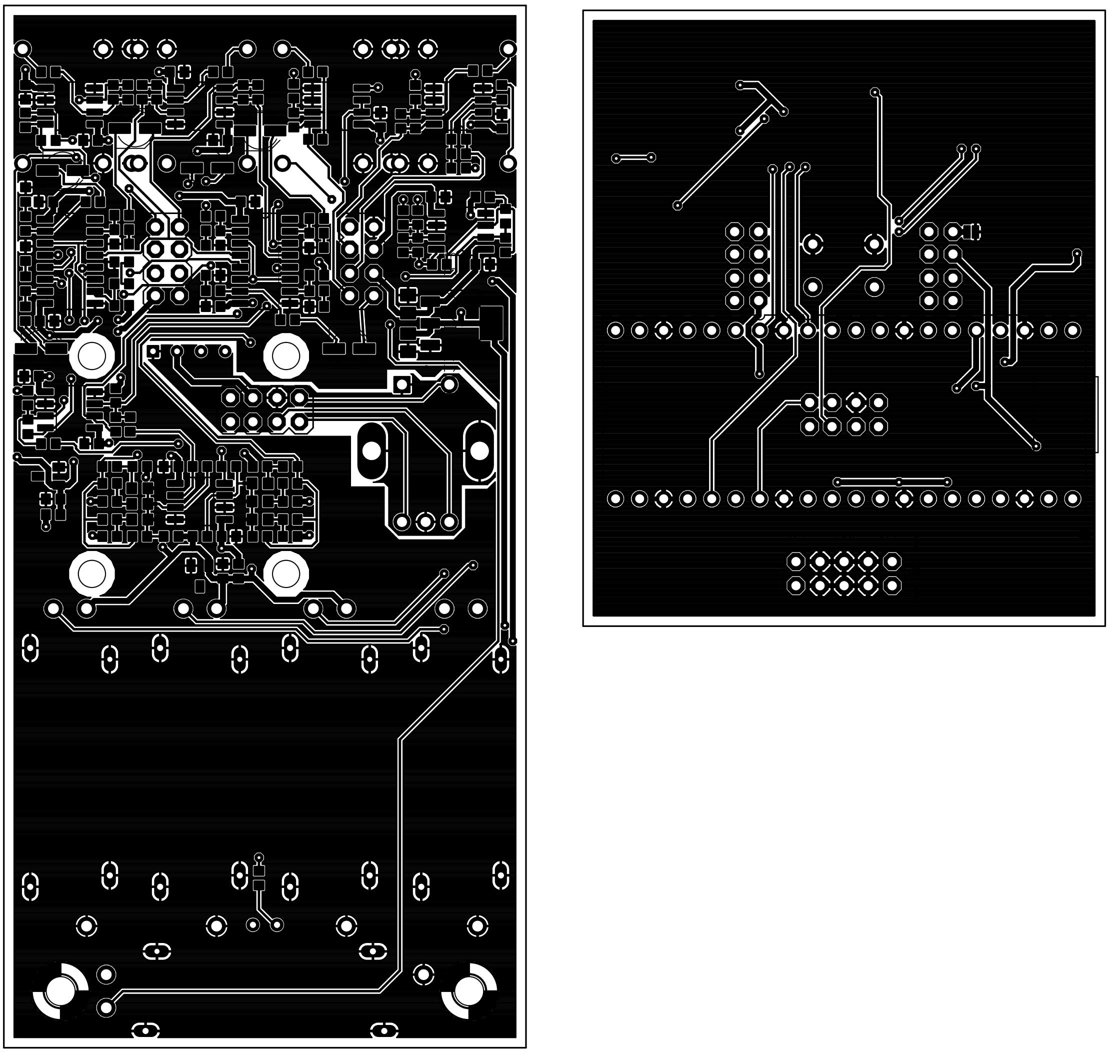

Fig. B.2: Bottom layer of the PCB

B.3 Assembly view – top

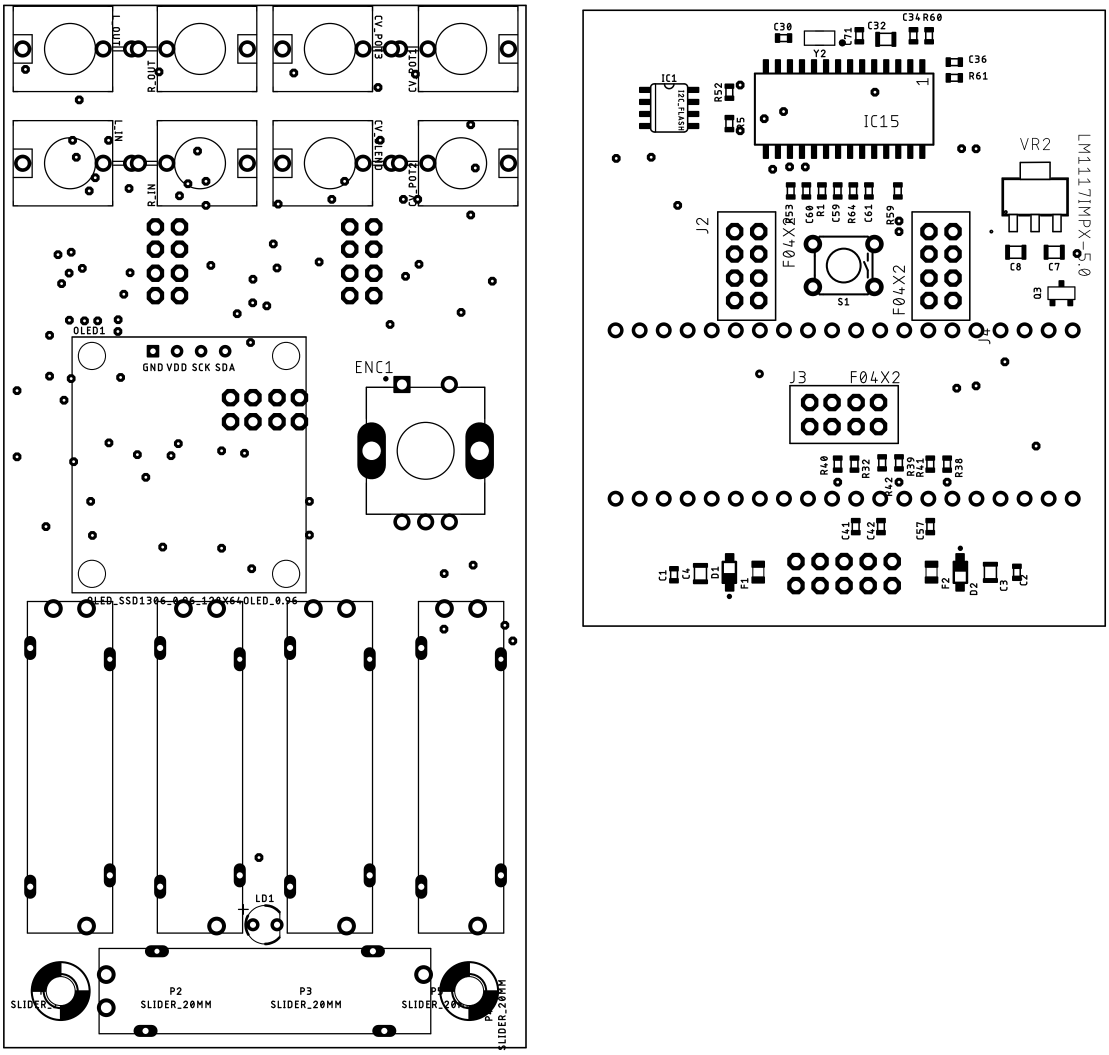

Fig. B.3: Top layer of the assembly view

B.4 Assembly view – bottom

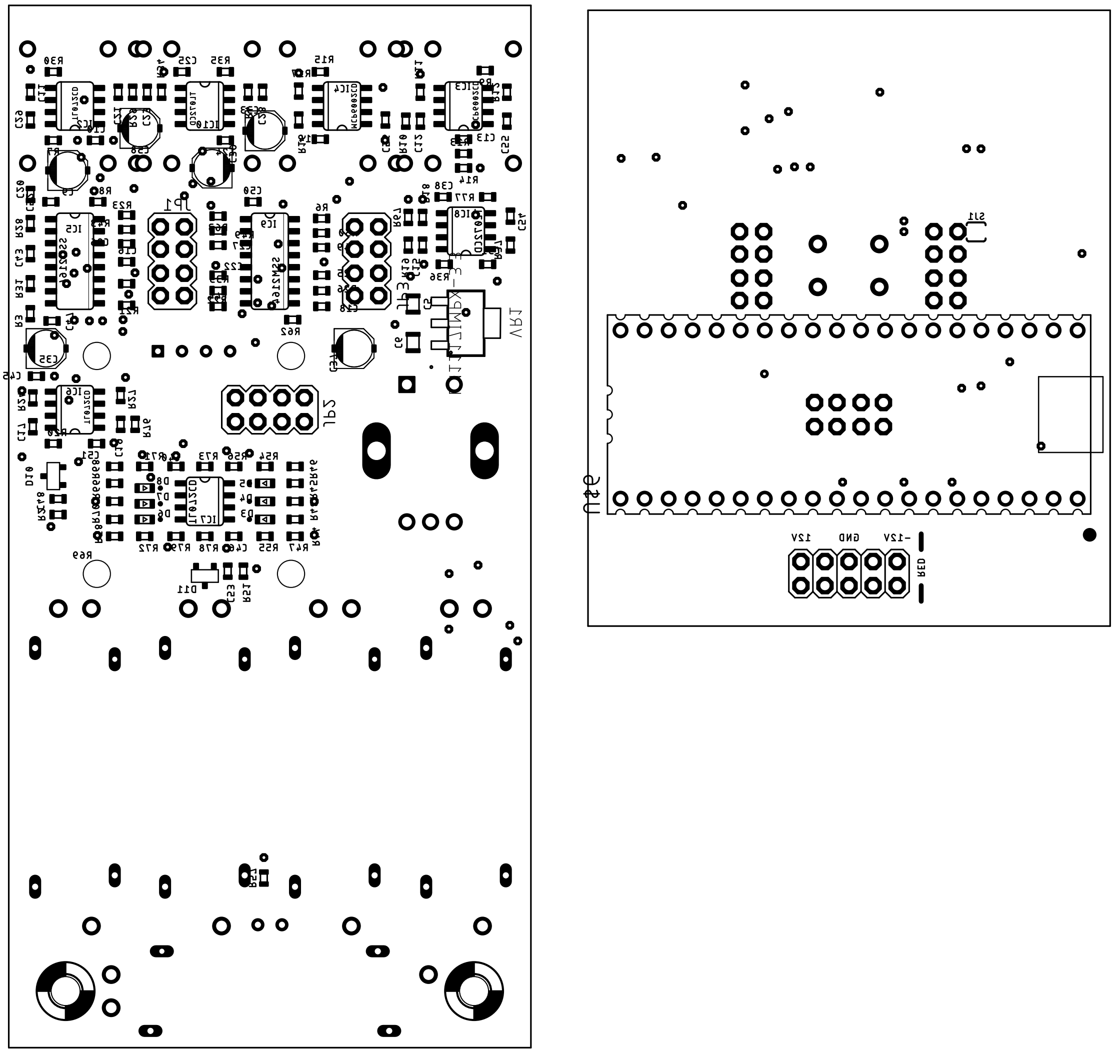

Fig. B.4: Bottom layer of the assembly view